

sized iron oxide (Fe_3O_4) with a surrounding polymer coating and become magnetized when placed in an external alternating magnetic field (AMF) [10]. In hyperthermia treatment, the expression of heat shock proteins (HSPs) plays an important role in immune reactions [11–19]. Accumulating evidence from our group [20–23] and from others [24] implicates HSP expression induced by hyperthermia in tumor immunity and opens the door to cancer therapy based on hyperthermia treatment (thermo-immunotherapy). In such a strategy, a tumor-specific hyperthermia system that can induce necrotic cell death via HSP expression without damaging noncancerous tissues would be highly desirable. An intracellular hyperthermia system using tumor-targeted magnetite nanoparticles facilitates tumor-specific hyperthermia; this can induce necrotic cell death via HSP expression, which in turn induces antitumor immunity.

We synthesized, in our initial study, magnetite cationic liposomes (MCLs) loaded with 4-S-cysteaminyphenol (CAP) [25]. There was, however, a risk of nonspecific electrostatic interaction between MCLs and various non-target cells. A promising technique is the use of tumor-targeted magnetite nanoparticles, and this approach is extended by synthesizing another type of magnetite nanoparticles, NPrCAP/M, on which NPrCAP is superficially and directly bound on the surface of magnetite nanoparticles. NPrCAP/M is chemically stable and can be produced in large quantities and employed to effect melanoma-targeted chemotherapy (by NPrCAP) and thermoimmunotherapy (by magnetite with HSP). In this study, we evaluated their thermo-therapeutic effect on distant metastatic melanomas, using the mouse B16 melanoma system. Specifically we assessed the *in vivo* growth inhibition of a subsequently transplanted melanoma growth (re-challenge melanoma) after treating the initial melanoma transplant. We also investigated the possible association of HSP production with growth inhibition of the re-challenge melanoma.

2. Materials and Methods

2.1. Preparation of NPrCAP/M. The details of the preparation of NPrCAP/M are described elsewhere [26]. Briefly, magnetite nanoparticles (Fe_3O_4 ; average particle size, 10 nm) were coated with aminosilane and conjugated with NPrCAP via maleimide cross-linkers. The resultant NPrCAP/M was suspended in 10 mL of H_2O . The degree of incorporation of NPrCAP to magnetite was 61.0 nmol/mg magnetite.

2.2. Cells and Animal Models. All of the animal experiments were conducted by an approval of Animal Experiment Ethics Committee of Sapporo Medical University. All the surgical, transplantation and drug administration procedures were carried out after anesthesia by diethyl ether. Mouse B16F1 and B16F10 and B16 OVA melanoma cells (3.0×10^5) in 0.1 mL of phosphate-buffered saline (PBS) were *s.c.* transplanted into the right flanks of 4-week-old female C57BL/6 mice (weighing approximately 10.0 g and purchased from Hokudo Laboratory, Sapporo, Japan). B16F1 and B16F10 cells were purchased from ATCC (Summit Pharmaceuticals

Intl. Corp., Tokyo, Japan). B16OVA is a B16F1 melanoma cell line stably transfected with chicken ovalbumin (OVA) cDNA and was kindly provided by Dr. Y. Nishimura, Kumamoto University, Kumamoto, Japan [27]. On day 5 after transplant mice with primary melanoma transplantation were randomly divided into treatment groups. With a 26-gauge microsyringe, the B16 melanoma-bearing mice were injected with 0.1 mL of NPrCAP/M (40.0 mg/mL solution) directly into the tumor site in a single-dose administration (approximately $0.5 \mu\text{L}/\text{mm}^3$ tumor volume). Treated tumors on the right flank in mice were excised on day 13 after the first *s.c.* transplantation. On day 40 after the surgical excision (on day 53 after primary transplantation), mice were re-challenged with 1.0×10^5 B16 cells which were injected into the left flank. The total number of melanoma cells at the re-challenge experiments was 1/3 of melanoma cells as that of the primary transplants because there was no NPrCAP/M administration which might cause some tissue destruction. The control group, naive mice of the same age and sex, received transplantation of melanoma cells into the right flank as with the treated groups. On day 14 after the secondary transplantation (day 67 after primary transplantation), tumor diameters were measured in millimeters with calipers, and tumor volumes were calculated by the formula: long axis \times (short axis)² \times 0.5. The mice in the treated groups were judged to be tumor free (rejection) if the tumor was less than about 2 mm in diameter by palpation on day 60 after the secondary transplantation (day 113 after the primary transplantation).

2.3. Magnetite-Nanoparticle-Mediated Hyperthermia. An alternating magnetic field (AMF) was generated using a horizontal coil (inner diameter: 7 cm; length: 7 cm) with a transistor inverter (LTG-100-05; Dai-ich High-Frequency Co., Tokyo, Japan). The magnetic field frequency and intensity were 118 kHz and 30.6 kA/m (384 Oe), respectively. Mice were exposed to the AMF inside the coil for 15 or 30 minutes. Surface (peripheral) and core (central) temperatures of the tumor were continuously monitored and measured using two optical fiber probes (FX-9020; Anritsu Meter, Tokyo, Japan); that is, one inserted into the tumor core and another fixed on the tumor surface. Measurement time points were 0, 1, 2, 3, 4, 5, 10, 15, 20, 25, 30, 31, 32, 33, 34, and 35 minutes for 30 minutes thermotherapy. The therapeutic temperatures at 41 C, 43 C or 46 C were monitored by measuring the surface temperature and adjusting the transistor inverter during exposure to AMF (Figures 1(a), 1(b), and 1(c)).

2.4. Treatment Protocols. Animal experiments were carried out using the four protocols described below. Each experimental group of Protocols number 1 through number 4 consisted of six to eleven mice. All the treatment protocols were again approved by the Animal Experimental Ethics Committee of Sapporo Medical University. The experimental conditions for melanoma transplantation and the methods of NPrCAP/M administration were identical in all four protocols and all the animal experiments including drug

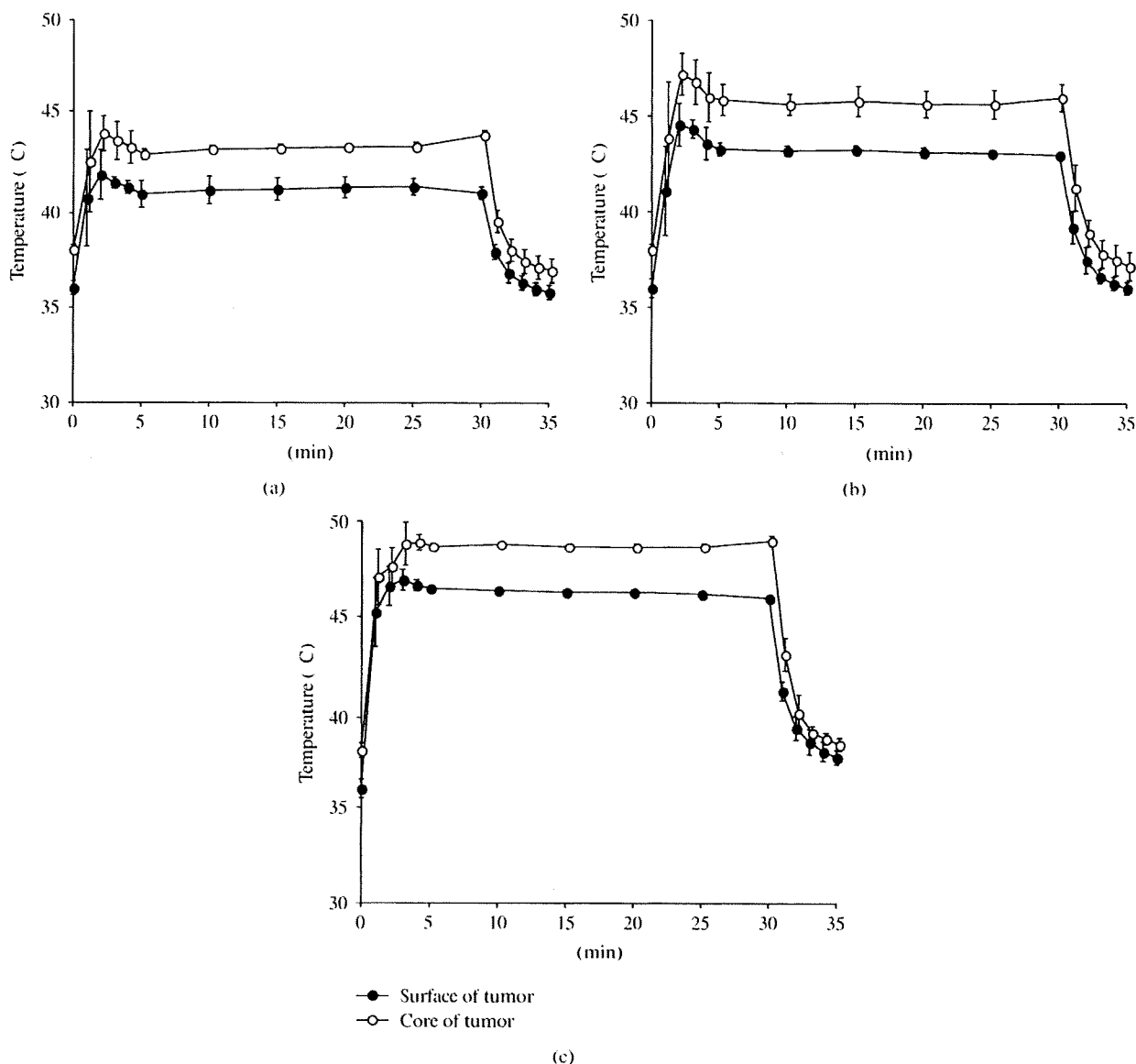


Figure 1: Shifts of temperatures at the core and the surface of tumors during AMF exposure. The temperature at the tumor surface was maintained at 41 C (a), 43 C (b), and 46 C (c) for 30 minutes by adjusting the power of the AMF generator. Temperatures of both the tumor surface and core were measured simultaneously.

administration were carried out after anesthesia by diethyl ether.

2.4.1. Protocol Number 1: Effect of NPrCAP/M with and without AMF on Re-Challenge Tumor Growth. On day 5 after the s.c. transplantation of B16 melanoma cells, mice were divided into four groups. In Groups I and II mice received s.c. administration of 0.1 mL of 40.0 mg/mL aminosilane-coated magnetite (M) once a day every other day for a total of three days (days 6, 8, and 10) with AMF (Group II) or without AMF (Group I). In Groups III and IV mice

received s.c. administration of 0.1 mL of NPrCAP/M (4.0 mg magnetite equivalent) once a day every other day for a total of three days (days 6, 8, and 10) with (Group IV) or without (Group III) AMF. The temperature at the tumor surface was maintained at 43 C during exposure for 30 minutes by controlling AMF intensity. Mice of a control group of the same age and sex received s.c. transplantation of melanoma cells into the right flank, as with the treated groups. On day 13 after the primary transplantation all mice underwent total resection of melanoma nodules. On day 53 after the first transplantation (postoperative day 40), surviving mice in each group received a second transplantation of B16

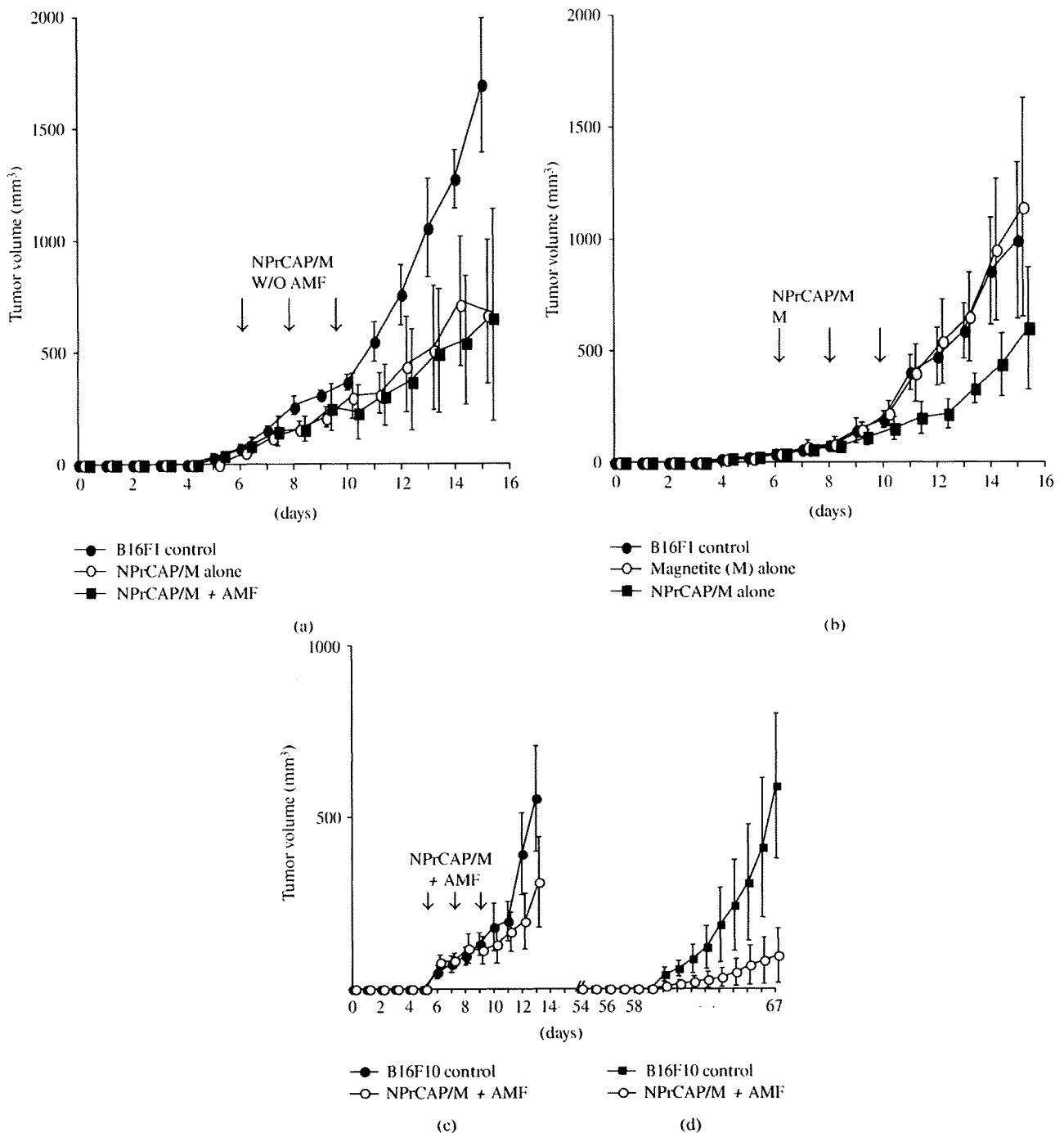


Figure 2: Growth curves of primary B16 melanomas. Experimental conditions and statistical analyses of (a), (b), (c) and (d) are identical to those of Protocol number 1. (a) Growth curve of B16F1 melanoma cells treated with NPrCAP/M alone without heat ($n = 10$) and with heat by AMF exposure ($n = 10$) at days 6, 8, and 10. These two groups showed a significant growth inhibition compared to that of control naive mice ($n = 10$) by Dunnet's test ($P < .01$). Importantly, there is no significant difference between the two groups with and without AMF exposure. (b) Growth curve of B16F1 melanoma cells treated with magnetite alone ($n = 10$) and NPrCAP/M alone without AMF exposure ($n = 10$). Mice with magnetite alone did not show any growth inhibition whereas NPrCAP/M alone resulted in a significant growth inhibition of primary melanoma ($P < .01$). (c) Comparison of growth inhibition of B16F10 primary melanomas after treatment with NPrCAP/M with AMF exposure. Compared to control naive mice ($n = 10$) transplanted with B16F10 cells without any treatment, those mice ($n = 10$) with NPrCAP/M plus AMF exposure showed a significant growth inhibition of primary B16F10 melanomas with a similar degree to that of B16F1 melanoma (Figure 2(a)) ($P < .01$ by Dunnet's test). (d) Comparison of the growth inhibition of B16F10 secondary, re-challenge melanoma. The mice ($n = 10$) with NPrCAP/M plus AMF exposure showed a marked growth inhibition compared to control naive mice without any treatment ($n = 10$).

melanoma cells into the opposite flank. Tumor volumes were calculated at day 14 after the second transplantation of B16 melanoma cells.

2.4.2. Protocol Number 2: Effect of Treatment Frequency with NPrCAP/M on Re-Challenge Tumor Growth. Mice were randomly divided into six treatment groups. They were exposed to AMF once on day 6 (Group I), twice (on days 6 and 8) (Group II), twice (on days 6 and 10) (Group III), three times (on days 6, 8, and 10) (Group IV), three times (on days 6, 7, and 8) (Group V), and five times (on days 6 through 10) (Group VI).

2.4.3. Protocol Number 3: Effect of Temperature and Treatment Frequency of NPrCAP/M with AMF on Re-Challenge Tumor Growth. Mice were divided into six groups. Mice of Groups I and II were exposed to the AMF to maintain the surface temperature at 41 °C once a day for two days (days 6 and 10) and for three days (days 6, 8, and 10), respectively. Using the same day schedule mice of Groups III and IV were exposed to the AMF at 43 °C and mice of Groups V and VI at 46 °C.

2.4.4. Protocol Number 4: Effect of Temperature and Treatment Duration on Re-Challenge Tumor Growth. Mice were divided into four groups. Temperatures at the surface of the tumors in Groups I and II were maintained at 43 °C and 46 °C, respectively, during AMF exposure for 15 minutes. The surface temperatures in Groups III and IV were maintained at 43 °C and 46 °C, respectively, during therapy for 30 minutes.

2.5. ELISA for Heat Shock Protein 70 (HSP70) Expression in a Tumor. After thermotherapy, the amount of HSP70 in the primary tumor was measured using an HSP70 EIA Kit (Stress Gen Biotechnologies, British Columbia, Canada) according to the manufacturer's instructions. The total protein content of the tumor homogenates was determined using the BCA Protein Assay Kit (Pierce Biothechnology, Inc., USA). The control group was composed of mice without NPrCAP/M administration or AMF exposure. Group I received s.c. administration of NPrCAP/M directly at the tumor site once a day without AMF exposure. Mice of Groups II and III received thermotherapy at 41 °C for 15 minutes and 30 minutes, Groups IV and V at 43 °C for 15 minutes and 30 minutes, and Groups VI and VII at 46 °C for 15 minutes and 30 minutes, respectively. Then, 24 hours later, all tumors were removed, and their lysates were processed for the HSP70 assay. In separate groups, tumors were excised at 24, 48, and 72 hours after the 43 °C thermotherapy for 30 minutes, and amounts of HSP70 were measured.

2.6. Histological and Immunohistochemical Study. After thermotherapy in the primarily transplanted melanoma at 43 °C for 30 minutes once a day for three days (Figure 4(a), Group IV), melanomas in re-challenge mice were excised on the 18th day after second transplantation of B16F1 cells. Para n-embedded sections were prepared and processed for

HE staining. The frozen tumor tissues were stained with antimouse CD4 (Santa Cruz Biotechnology Inc., CA, USA) or CD8 (Chemicon International Inc., CA, USA).

2.7. Statistical Analysis. Data were analyzed by one- or two-way analysis of variance (ANOVA), and then differences in experimental results for tumor growth and expression of HSP were assessed by She e's test to compare all the experimental groups, or by Dunnett's test, which compared the experimental versus the control groups. Differences in survival rates were analyzed by the Kaplan-Meier method and log-rank test with Bonferroni correction for multiple comparisons. The level of significance was $P < .05$ (two-tailed). All statistical analyses were performed using Stat View J-5.0 (SAS Institute Inc. Cary, NC).

3. Results and Discussion

In the search for successful cancer treatment it is self-evident that the exploitation of a specific biological property is one of the best approaches for developing the targeted therapy [27, 28]. We have previously shown that the melanogenesis substrate, NPrCAP, is a good candidate for developing melanoma chemotherapy because melanogenesis is uniquely expressed in melanocytic cells and is inherently cytotoxic from the action of tyrosinase on tyrosine with formation of highly reactive free radicals [1, 4]. Nanoparticles may also provide a good platform to coadminister anti-cancer therapeutics directed at different targets. Specifically hyperthermia with the use of magnetite nanoparticles has been shown to possess great potential to develop thermo-immunotherapy [23, 29]. In this study the conjugate of NPrCAP and magnetite nanoparticles, NPrCAP/M was synthesized with the hope of developing a chemotherapeutic as well as a thermo-immunotherapeutic effect. We employed two cell lines of B16 melanoma, that is, B16F1 and B16F10, and B16OVA cells and compared the thermo-therapeutic protocols in detail by evaluating the growth of the re-challenge melanoma as well as the duration and rates of survival of melanoma-bearing mice.

3.1. Immediate and Steady Generation of Heat by Intratumor Administration of NPrCAP/M with AMF Exposure on B16 Melanoma Nodules. In the previous intratumor MCL hyperthermia for B16 melanoma the skin surface temperature above the subcutaneous tumor rose to 43 or 46 °C [29]. To obtain a rapid and steady temperature increase at the core and the surface of the B16 melanoma, NPrCAP/M was injected into the center of the tumor nodules, and internal and surface tumor temperatures were measured during AMF exposure. Both temperatures increased within one minute to the target of 41 °C, 43 °C, or 46 °C (Figures 1(a), 1(b), and 1(c)), indicating that NPrCAP/M injection followed by AMF exposure could immediately and steadily heat the subcutaneously transplanted melanoma nodules. The temperature at the tumor center was approximately 2 °C higher than that at the tumor surface.

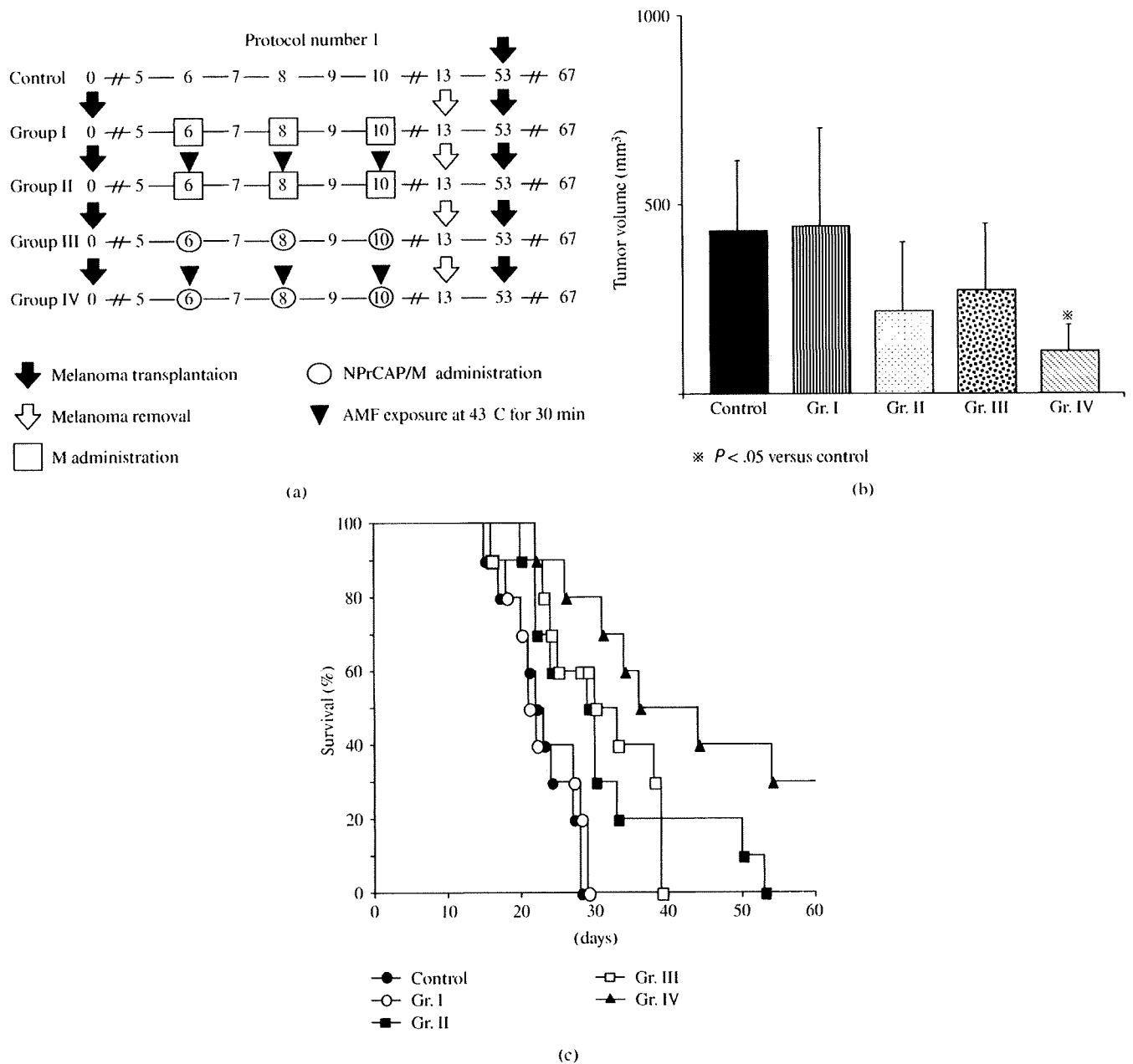


Figure 3: Time schedules and results for tumor volumes, survival periods, and rates of mice treated by the Protocol number 1. (a) Protocols of Groups I, II, III, and IV. (b) Tumor volumes of re-challenge B16F1 melanoma on day 14. All data are presented as mean ± standard deviation. Tumor volumes of Group IV were significantly reduced compared with those of the control group ($P = .0295$) or Group I ($P = .0215$). There were no significant interactions between drugs and AMF ($P = .5568$). (c) Kaplan-Meier survival curve over a period of 60 days after tumor re-challenge in Protocol number 1.

3.2. *E ective and Equal Inhibition of B16 Melanoma Growth at the Site of Primary Transplantation by Intratumor Administration of NPrCAP/M with and without Heat.* We first evaluated the chemotherapeutic e ect of NPrCAP/M with or without heat. NPrCAP/M without heat inhibited the growth of primary transplants to the same degree as did NPrCAP/M with heat, indicating that NPrCAP/M alone has a chemotherapeutic e ect. The critical temperature for thermotherapy was documented to be 43 C for various

cell lines [7, 8]. Using two melanoma cell lines, B16F1, and B16F10 and B16OVA, we examined melanoma growth inhibition by intra-tumor administration of NPrCAP/M into primary tumors on days 6, 8, and 10 after transplantation with exposure to AMF at 43 C for 30 minutes (Figures 2(a) and 2(c)) under the experimental conditions of Protocol number 1 (Figure 3(a)). Both NPrCAP/M with and without AMF exposure resulted in a significant and equal reduction of melanoma tumor volume in both B16F1 and F10 cells

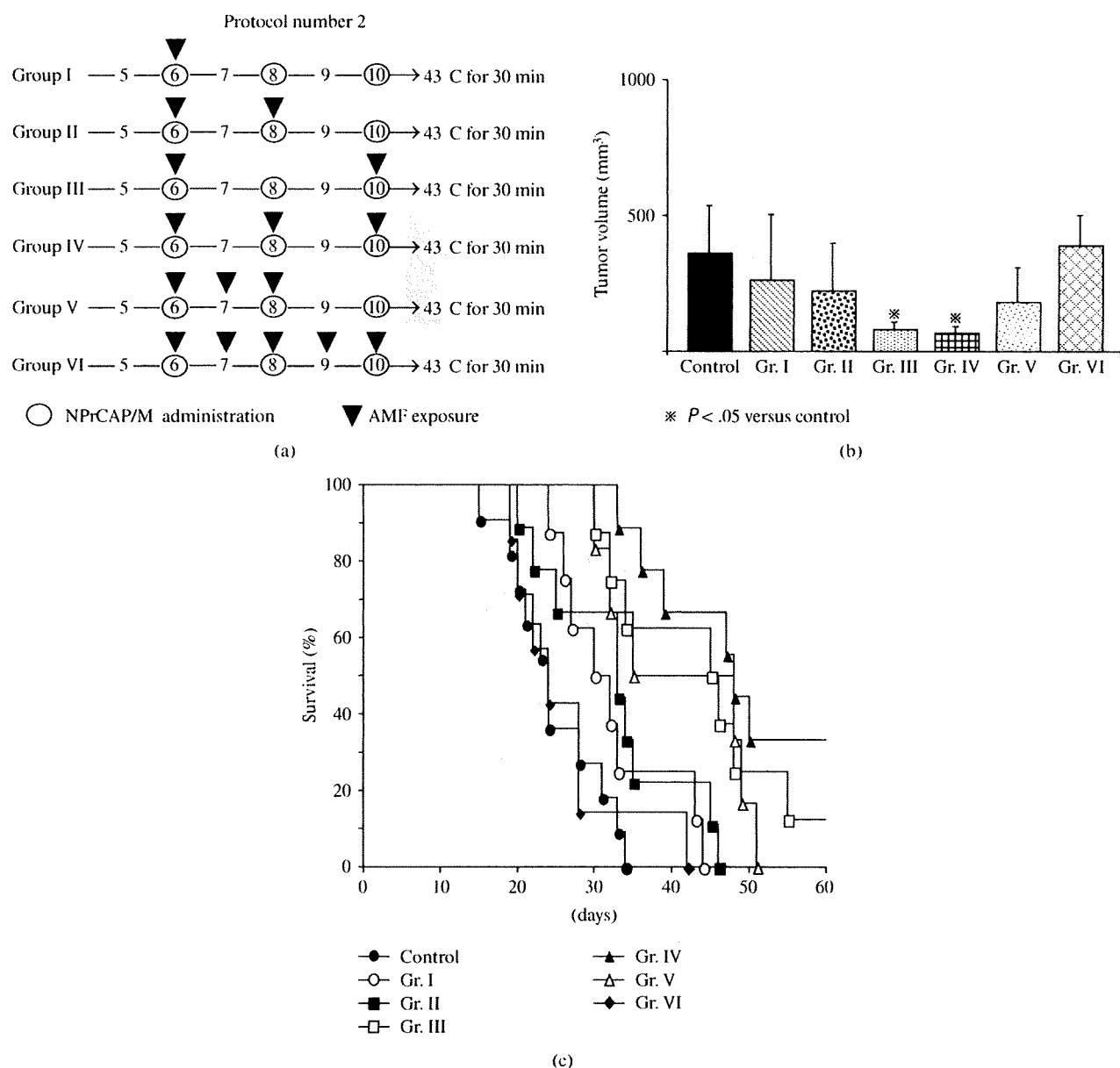


Figure 4: Time schedule and results for tumor volumes, survival periods, and rates of mice treated by Protocol number 2. (a) Protocols of Groups I, II, III, IV, V, and VI. (b) Tumor volumes on day 14 after re-challenge with B16F1 melanoma. All data are presented as mean \pm standard deviation. Tumor volumes of Groups III and IV were found to be significantly reduced compared with those of the control group ($P = .0411$ and $.0195$, resp.) and Group VI ($P = .0444$ and $.0237$, resp.) by the Scheffé test. (c) Kaplan-Meier survival curves over a period of 60 days after re-challenge with B16F1. The survival rate of Group III was significantly prolonged compared with those of the control group ($P = .0006$) and Group VI ($P = .0013$). The survival rate of Group IV was significantly prolonged compared with that of the control group ($P < .0001$), Group I ($P = .0014$), Group II ($P = .0014$), and Group VI ($P = .0013$). One of the eight mice in Group III and three of the nine mice in Group IV were protected against re-challenge with B16F1 melanoma cells.

at the site of primary transplantation ($P < .01$ by two-way repeated measure ANOVA, Figures 2(a) and 2(c)) compared to tumor volume of naive control mice. B16 OVA cells also gave the same experimental results (data not shown). Control studies comparing magnetite alone and magnetite plus NPrCAP (NPrCAP/M) without AMF

exposure showed that magnetite alone does not have any melanoma growth inhibiting effect whereas NPrCAP/M without AMF significantly inhibited melanoma-growth ($P < .01$ by two-way repeated measure ANOVA, Figure 2(b)). Since we obtained basically same growth inhibition results for both the primary and secondary transplants from the

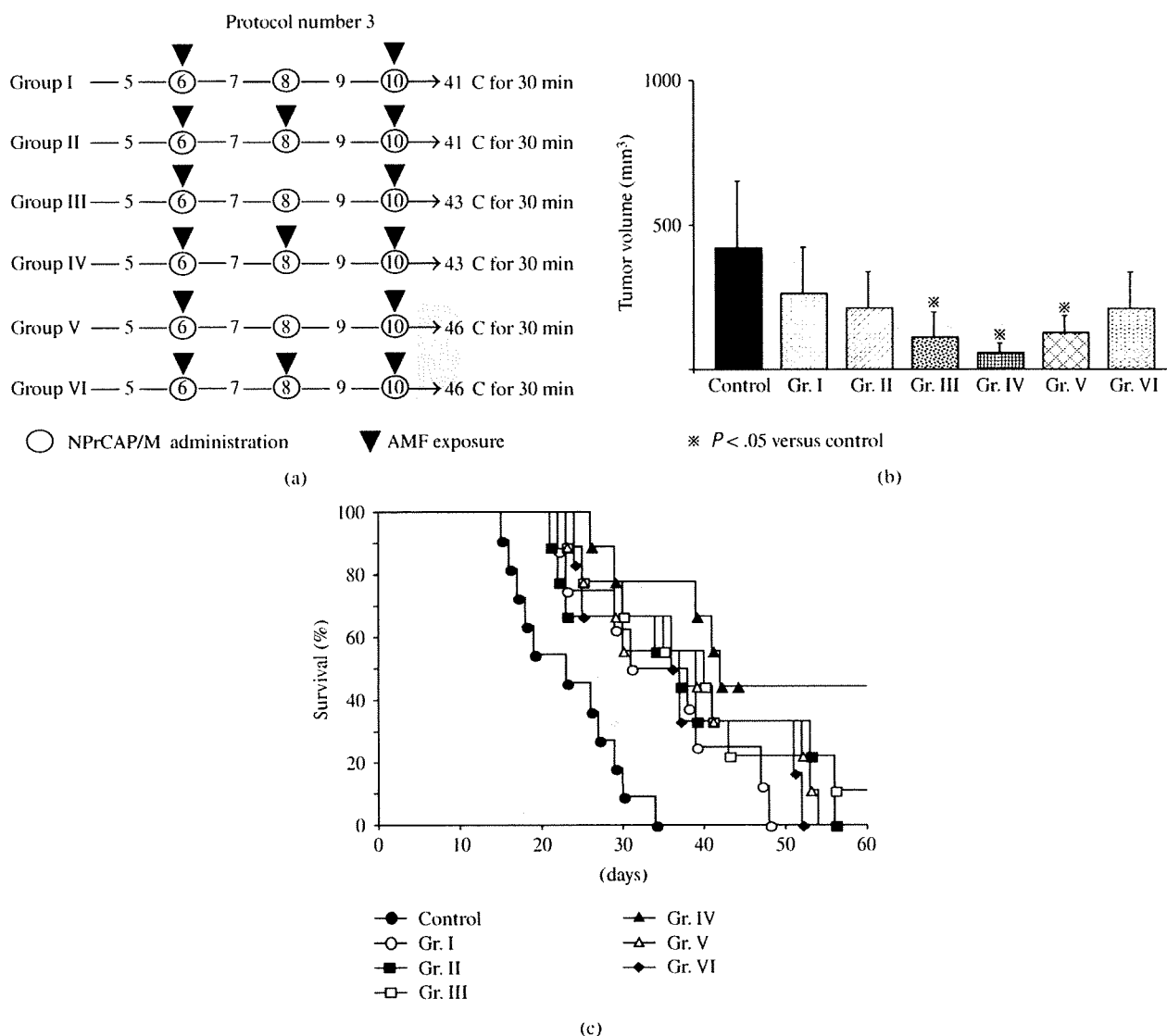


Figure 5: Time schedules and results for tumor volume, survival periods and rates of mice treated by Protocol number 3. (a) Protocols of Groups I, II, III, IV, V, and VI. (b) Tumor volumes on day 14 after re-challenge with B16F1 melanoma. All data are presented as mean ± standard deviation. Tumor volumes of Groups III, IV, and V were significantly reduced compared with the control group ($P = .0045, .0004, \text{ and } .0085$ resp.) by the Sche \acute{e} test. (c) Kaplan-Meier survival curve over a period of 60 days after tumor re-challenge. Survival rates of Groups III and IV were significantly prolonged compared with that of the control group ($P = .0011$ and $.0002$, resp.). One of the nine mice in Group III and four of the nine mice in Group IV were protected against re-challenge with B16F1 melanoma cells.

two cell lines, the majority of subsequent studies listed in Protocols number 1 through number 4 were conducted on B16F1 cells.

3.3. *E ffective Growth Inhibition of B16F1 Melanoma Cells at the Site of Re-Challenge, Second Transplantation by NPrCAP/M with AMF Exposure (Protocol number 1).* We then evaluated whether NPrCAP/M treatment with or without heat in the local primary tumor could inhibit the growth of distant tumors which were not given an intra-tumor injection of NPrCAP/M. There was a significant

difference in the melanoma growth inhibition of re-challenge transplants between the groups of NPrCAP/M with and without heat. NPrCAP/M with AMF exposure showed the most significant growth inhibition in re-challenge melanoma and increased life span of the host animals, that is, 30%–50% complete growth inhibition (rejection) of re-challenge melanoma growth, indicating that NPrCAP/M with heat possesses a thermo-immunotherapeutic effect. For this, we treated the primary B16F1 and F10 melanoma cells by NPrCAP/M and then measured the volume of the secondary melanoma after the second transplantation at a different site to the first transplant. We also evaluated the survival periods

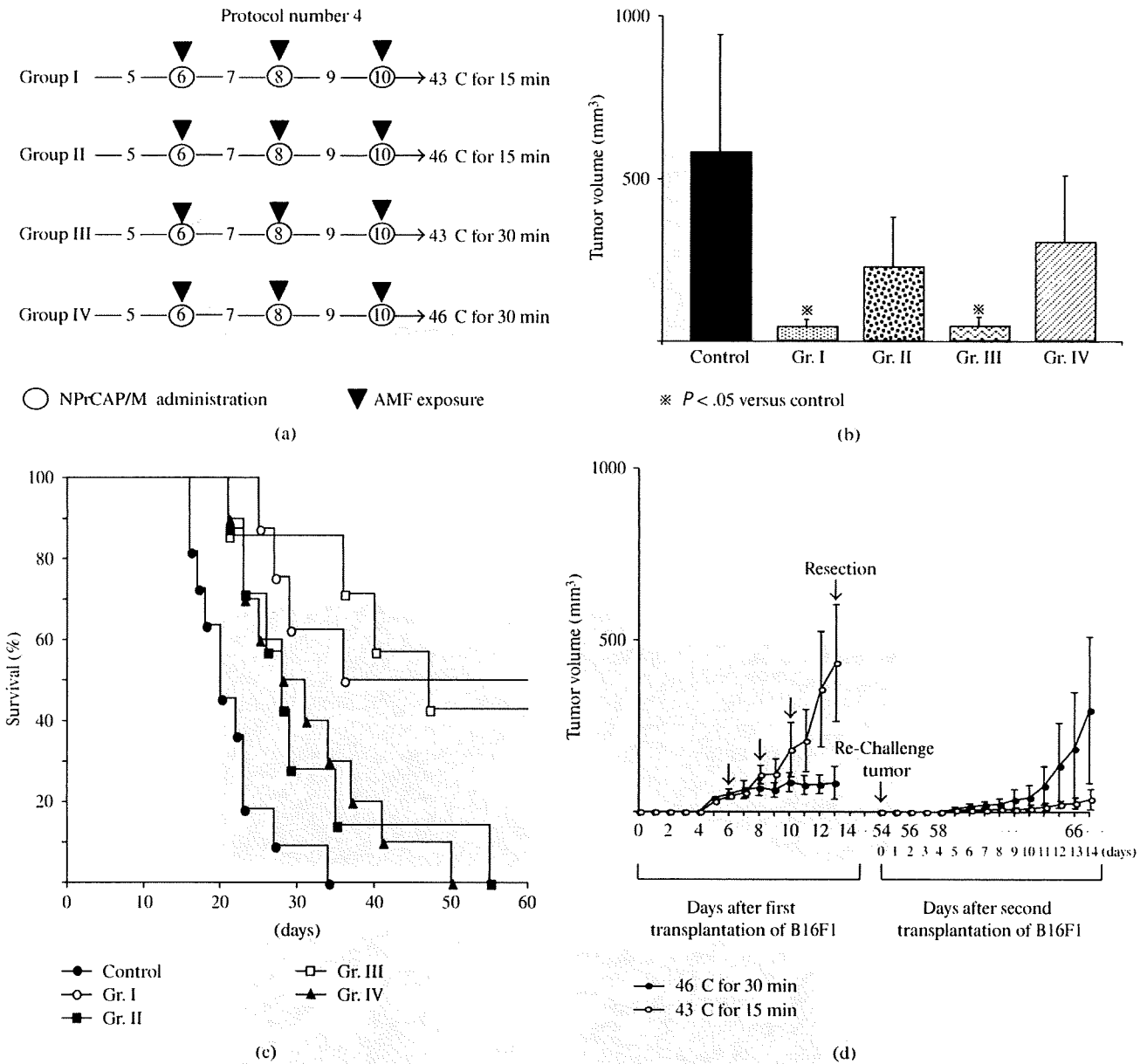


Figure 6: Time schedules and results for tumor volumes, survival periods, and rates for treatment with Protocol number 4. (a) Protocols of Groups I, II, III, and IV. (b) Tumor volumes on day 14 after re-challenge with B16F1 cells. All data are presented as mean ± standard deviation. Tumor volumes of Groups I and III on day 14 were significantly reduced compared with that of the control group ($P = .0009$ and $.0016$, resp.) by Scheffé test. (c) Kaplan-Meier survival curve over a period of 60 days after re-challenge. Survival rates of Group I and III were significantly prolonged compared with that of the control group ($P = .0004$ and $.0005$, resp.). Four of the eight mice in Group I and three of the seven mice in Group III were protected against re-challenge with B16F1 melanoma cells. (d) Tumor volumes of the primary tumor and re-challenge tumor as representative examples of Groups I ($n = 8$) and IV ($n = 10$) which were treated at 43 C for 15 minutes and 46 C for 30 minutes, respectively. All data are presented as mean ± standard deviation.

and rates of host melanoma-bearing mice. These secondary melanomas were not directly exposed to NPrCAP/M; hence we could evaluate the thermo-immunotherapeutic effect of NPrCAP/M treatment.

First, we compared the therapeutic effects among Groups I (intratumor injection of magnetite nanoparticles alone

without AMF exposure), II (magnetite injection and heat at 43 C for 30 minutes by AMF), III (NPrCAP/M injection without AMF), and IV (NPrCAP/M injection and heat at 43 C for 30 minutes by AMF) of Protocol number 1 (Figure 3(a)). As shown in Figure 3(b), NPrCAP/M-mediated hyperthermia at 43 C showed the most significant

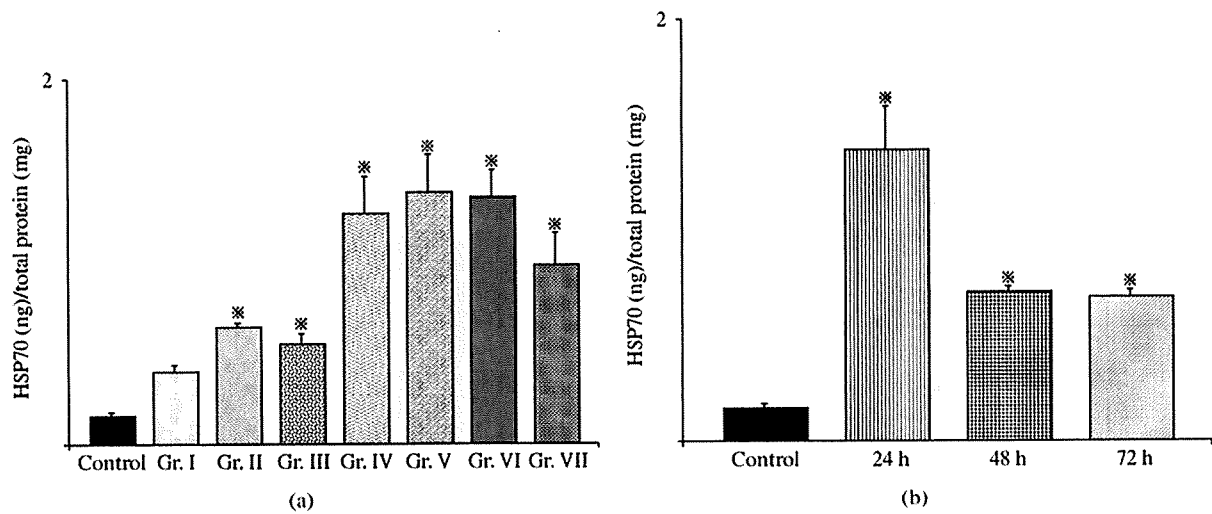


Figure 7: Expression of HSP70 in a tumor after thermotherapy. (a) Amounts of HSP70 in tumors 24 hours after thermotherapy as described in the Materials and Methods. All data are presented as mean \pm standard deviation ($n = 4$). There were significant differences between the control group and all other groups except Group I by Dunnett's test ($P < .05$). (b) Amounts of HSP70 24, 48, and 72 hours after thermotherapy at 43 C for 30 minutes. All data are presented as mean \pm standard deviation ($n = 4$). There were significant differences between the control group and all other groups by Dunnett's test ($P < .05$).

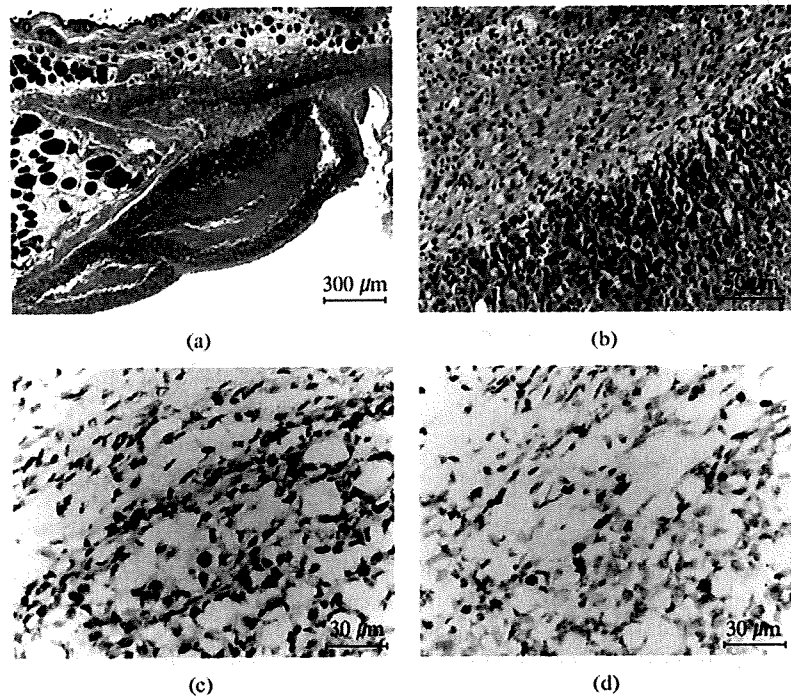


Figure 8: Histopathology and immunohistochemistry of a re-challenge tumor. (a) A low-power view of a re-challenge tumor with HE staining ($\times 40$). (b) A high-power view ($\times 200$). Monocytic infiltrates are seen around a necrotic lesion. (c) CD4⁺ T cells ($\times 400$). (d) CD8⁺ T cells ($\times 400$). Almost equal numbers of CD4⁺ and CD8⁺ T cells are observed.

growth inhibition of secondary B16F1 melanoma in re-challenged mice. Both magnetite nanoparticles with heat at 43 C and NPrCAP/M without heat also inhibited the growth of secondary melanomas, though statistically not significant (Figure 3(b) and (c)). Most importantly, NPrCAP/M

alone without heat caused equal growth inhibition of secondary melanomas to that induced by magnetite with AMF exposure, suggesting some immunotherapeutic effect of NPrCAP/M. A similar growth inhibition of secondary transplanted melanoma cells was obtained in B16F10 (Figure 2).

Next, we compared the life span of the host animals among 4 groups. The survival of mice in Group IV was prolonged, compared with that of the control group ($P = .0003$) and Group I ($P = .0003$). Three of the ten mice in Group IV (30%) were protected completely from re-challenge with B16F1 cells (Figure 3(c)). Magnetite alone with AMF exposure at 43 C (Group II) and NPrCAP/M alone without heat (Group III) failed to show any statistically significant prolongation of the host animal survival.

3.4. Effect of Treatment Frequency for the Primary Tumor on Growth Inhibition of Re-Challenge Melanoma (Protocol number 2). To evaluate the effect of the number of treatments for the primary tumor on the re-challenge tumor, six treatment approaches were designed using B16F1 cells. They consisted of hyperthermia once on day 6 (Group I), twice on days 6 and 8 (Group II) or days 6 and 10 (Group III), three times on days 6, 8, and 10 (Group IV) or 6, 7, and 8 (Group V), and a total of five times on days 6 through 10 (Group VI) (Figure 4(a)). Melanoma tumor volumes in re-challenged mice were smallest in Groups III and IV, while the longest survival periods and rates were obtained in Group IV with complete growth inhibition (rejection) of second re-challenge being 33% ($n = 9$) on day 60 (Figures 4(b) and 4(c)). The consecutive irradiation on days 6, 7, and 8 (Group V) or days 6 through 10 resulted in larger volumes of secondary tumors and poorer survival periods and rates compared to Group III or IV (Figures 4(b) and 4(c)). These findings suggested that repeated hyperthermia, once a day every other day for a total of three days, could induce effective degradation of B16 melanoma cells, which then most likely induced host immunity against melanoma.

3.5. Effect of Temperature and Treatment Frequency on Melanoma Growth Inhibition in Re-Challenge Mice (Protocol number 3). Our study indicated that the most effective thermo-immunotherapy for re-challenge B16 melanoma can be obtained at a temperature of 43 C for 30 minutes with the treatment repeated three times on every other day intervals without complete degradation of the primary melanoma. We compared growth inhibition of secondly transplanted melanomas at therapeutic temperatures of 41 C, 43 C, and 46 C for 30 minutes twice on days 6 and 10, or three times on days 6, 8, and 10 (Figure 5(a)). As shown in Figures 5(b) and 5(c), thermotherapy at 43 C in Group IV (43 C, every other day for a total of three times on three days) was the most effective for the growth inhibition of both the secondly transplanted, re-challenge melanoma and for improving the survival rates and duration of host mice. Four of the nine mice in Group IV (44.4%) were protected completely against re-challenge with B16F1 melanoma on day 60 (Figure 5(c)).

Our therapeutic conditions and their effects differ from those of magnetically mediated hyperthermia on the transplanted melanomas reported previously [29]. MCL-mediated hyperthermia for B16 melanoma showed that hyperthermia at 46 C once or twice led to regression of 40%–90% of primary tumors and to 30%–60% survival

of mice, whereas hyperthermia at 43 C failed to induce regression of the secondary tumors with 0% survival of mice [29].

3.6. Effect of Temperature and Treatment Duration on Melanoma Growth Inhibition in Re-Challenge Mice (Protocol number 4). We then compared the effects of temperature and duration of NPrCAP/M-mediated hyperthermia at 43 C for 15 minutes, 43 C for 30 minutes, 46 C for 15 minutes, and 46 C for 30 minutes on the re-challenge with B16F1 melanoma (Figure 6(a)). Tumor volumes and survival rates and periods of treatment of mice clearly showed that hyperthermia at 43 C elicited a more significant effect than that at 46 C (Figures 6(b) and 6(c)). Four of the eight mice (50%) in Group I (43 C for 15 minutes) and three of the seven mice (42.8%) in Group III (43 C for 30 minutes) survived 60 days after a second transplantation of B16F1 (Figure 6(c)), suggesting that NPrCAP/M with heat to the primary melanoma at 43 C for 15–30 minutes inhibits significantly the growth of distant metastatic melanoma, complete growth inhibition (rejection) of the second re-challenge melanoma being 42%–50%. Hyperthermia at 46 C for 30 minutes strongly inhibited the growth of the B16F1 tumor but had little effect on the re-challenge tumor, whereas hyperthermia at 43 C for 15 minutes hardly inhibited the growth of the primary tumor but strongly inhibited that of the second re-challenge tumor (Figure 6(d)). These findings suggest that NPrCAP/M-mediated hyperthermia at 43 C can be used most effectively to treat distant metastatic melanoma.

3.7. Production of HSP70 by NPrCAP/M Treatment and Presence of CD8⁺ T Cells around and within the Re-Challenge Melanoma. Heat shock protein forms a complex with intracellular peptides released from degrading tumor cells and presented by the MHC class I molecules of professional antigen-presenting cells [23]. We analyzed HSP70 production in the primary tumor and CD4⁺ and CD8⁺ T cell infiltration into the re-challenge secondary tumor. Figure 7(a) shows the amounts of HSP70 in the tumors at 24 hours after the NPrCAP/M-mediated hyperthermia. Among the six treatment groups, conditions of hyperthermia at 43 C for 15 or 30 minutes and 46 C for 15 minutes were equally effective for induction of HSP70 as those at 41 C for 15 minutes or 30 minutes and at 46 C for 30 minutes (Figure 7(a)). We also investigated whether expression of HSP70 in the posttherapeutic tumors depended on the duration of AMF exposure (15 minutes or 30 minutes), heating temperature (41 C, 43 C, or 46 C), and time elapsed after exposure (24 hours, 48 hours, or 72 hours). Figure 7(b) shows that the amount of HSP70 in the treated B16F1 tumors was most abundant at 24 hours after hyperthermia at 43 C, and over-expression of HSP70 was maintained at a significant level after 72 hours. Although thermotherapy at 46 C for 15 minutes could induce HSP70 as abundantly as that at 43 C for 30 minutes (Figure 7(a)), this condition failed to suppress the re-challenge melanoma transplant as

efficiently as 43 °C thermotherapy (Figures 5(b) and 5(c)). This suggests that immunological factors other than HSPs are at least in part responsible for growth inhibition and rejection of the re-challenge melanoma. Hyperthermia at 43 °C for 1 hour mediated the expression of MHC class I molecules after 24 hours in association with enhanced expression of HSP70 [30]. Heat treatment of tumor cells permits enhanced cross-priming, possibly via up-regulation of both HSPs and tumor antigen expression [24]. By inducing HSP70 and possibly MHC class I, immune T cells could aggregate around melanoma cells. We thus examined histochemically the immunological reaction against secondarily transplanted, re-challenge B16F1 melanoma in hematoxylin and eosin (HE)- and CD4- and CD8-stained sections. In addition to neutrophilic leukocytes, macrophages, and plasma cells, CD4⁺ and CD8⁺ T cells were observed around and within the re-challenge tumors with necrotic lesions (Figures 8(a), 8(b), 8(c), and 8(d)). These T cells were seen with a small number around the first transplant melanoma treated by NPrCAP/M with or without AMF exposure but hardly observed around the naive B16F1 tumors in mice that were not treated by NPrCAP/M-mediated thermotherapy (data not shown). This may indicate that melanoma-specific T cell immunity is likely involved in our NPrCAP/M therapy strategy.

4. Conclusions

This study has provided the basis for developing a melanoma targeted chemo-immuno-thermotherapy (CTI) strategy by conjugating melanogenesis substrate, NPrCAP with magnetite nanoparticles after exposure to alternating magnetic field. NPrCAP/M-mediated hyperthermia at a relatively low temperature (43 °C) effectively inhibited the growth of second transplant, re-challenge melanoma. Possibly, superficially bound NPrCAP possesses important roles in targeting nanoparticles to melanocytic cells and a chemotherapeutic effect on these cells. Based upon the present animal therapeutic protocol, that is, three-every-other-day treatment at 43 °C, we have started preliminary clinical trials (phase I/II) of NPrCAP/M CTI therapy with a significant success to a limited number of advanced stages III and IV melanoma patients. Four patients entered in this trial after approval of the Ethics Committee of Sapporo Medical University and two of them showed PR and CR, still surviving and carrying out normal daily life for more than 24 months [31].

Lastly, it should be noted that melanin intermediates produce reactive oxygen species such as superoxide and H₂O₂ [4, 32, 33]. This unique biological property of melanin intermediates not only causes cell death but also may produce immunogenic properties. In fact, NPrCAP/M alone without heat was as effective as magnetite nanoparticles with AMF exposure in inhibiting growth of re-challenge melanoma (Figures 3(b) and 3(c)). It would be interesting to know whether the growth of secondary re-challenge melanoma could be inhibited after treatment of NPrCAP alone onto the primary tumor [34]. The molecular background of our NPrCAP/M CTI therapy needs to be further studied.

Acknowledgments

The authors thank Toda Kogyo Co. (Hiroshima, Japan) and Meito Sangyo Co., Ltd. (Nagoya, Japan) for supplying magnetite nanoparticles and technical advice for the synthesis of NPrCAP/M, respectively. This work was supported by a Health and Labor Sciences Research Grant-in-Aid for Research on Advanced Medical Technology from the Ministry of Health, Labor and Welfare of Japan (H21-Nano-006). They wish to express their appreciation to Ms. Masae Okura for the technical help in conducting this research.

References

- [1] K. Jimbow, T. Iwashina, F. Alena, K. Yamada, J. Pankovich, and T. Umemura, "Exploitation of pigment biosynthesis pathway as a selective chemotherapeutic approach for malignant melanoma," *The Journal of Investigative Dermatology*, vol. 100, supplement 2, pp. 231S–238S, 1993.
- [2] F. Alena, T. Iwashina, A. Gili, and K. Jimbow, "Selective in vivo accumulation of N-acetyl-4-S-cysteaminylphenol in B16F10 murine melanoma and enhancement of its in vitro and in vivo antimelanoma effect by combination of buthionine sulfoximine," *Cancer Research*, vol. 54, no. 10, pp. 2661–2666, 1994.
- [3] J. M. Pankovich and K. Jimbow, "Tyrosine transport in a human melanoma cell line as a basis for selective transport of cytotoxic analogues," *Biochemical Journal*, vol. 280, no. 3, pp. 721–725, 1991.
- [4] K. Reszka and K. Jimbow, "Electron donor and acceptor properties of melanin pigments in the skin," in *Oxidative Stress in Dermatology*, J. Fuchs and L. Packer, Eds., pp. 287–320, Marcel Dekker, New York, NY, USA, 1993.
- [5] M. Tandon, P. D. Thomas, M. Shokravi, et al., "Synthesis and antitumor effect of the melanogenesis-based antimelanoma agent N-Propionyl-4-S-cysteaminylphenol," *Biochemical Pharmacology*, vol. 55, no. 12, pp. 2023–2029, 1998.
- [6] P. D. Thomas, H. Kishi, H. Cao, et al., "Selective incorporation and specific cytotoxic effect as the cellular basis for the antimelanoma action of sulphur containing tyrosine analogs," *The Journal of Investigative Dermatology*, vol. 113, no. 6, pp. 928–934, 1999.
- [7] O. Algan, H. Fosmire, K. Hynynen, et al., "External beam radiotherapy and hyperthermia in the treatment of patients with locally advanced prostate carcinoma," *Cancer*, vol. 89, no. 2, pp. 399–403, 2000.
- [8] M. D. Hurwitz, I. D. Kaplan, J. L. Hansen, et al., "Association of rectal toxicity with thermal dose parameters in treatment of locally advanced prostate cancer with radiation and hyperthermia," *International Journal of Radiation Oncology, Biology, Physics*, vol. 53, no. 4, pp. 913–918, 2002.
- [9] M. Johannsen, U. Gneveckow, L. Eckelt, et al., "Clinical hyperthermia of prostate cancer using magnetic nanoparticles: presentation of a new interstitial technique," *International Journal of Hyperthermia*, vol. 21, no. 7, pp. 637–647, 2005.
- [10] N. Kawai, A. Ito, Y. Nakahara, et al., "Anticancer effect of hyperthermia on prostate cancer mediated by magnetite cationic liposomes and immune-response induction in transplanted syngeneic rats," *Prostate*, vol. 64, no. 4, pp. 373–381, 2005.
- [11] S. Lindquist, "The heat-shock response," *Annual Review of Biochemistry*, vol. 55, pp. 1151–1191, 1986.

- [12] A. Konno, N. Sato, A. Yagihashi, et al., "Heat- or stress-inducible transformation-associated cell surface antigen on the activated H-ras oncogene-transfected rat fibroblast," *Cancer Research*, vol. 49, no. 23, pp. 6578–6582, 1989.
- [13] A. Ménoret and R. Chandawarkar, "Heat-shock protein-based anticancer immunotherapy: an idea whose time has come," *Seminars in Oncology*, vol. 25, no. 6, pp. 654–660, 1998.
- [14] P. K. Srivastava, A. Ménoret, S. Basu, R. Binder, and K. Quade, "Heat shock proteins come of age: primitive functions acquired new roles in an adaptive world," *Immunity*, vol. 8, no. 6, pp. 657–665, 1998.
- [15] Y. Tamura, N. Tsuboi, N. Sato, and K. Kikuchi, "70 kDa heat shock cognate protein is a transformation-associated antigen and a possible target for the host's anti-tumor immunity," *The Journal of Immunology*, vol. 151, no. 10, pp. 5516–5524, 1993.
- [16] Y. Tamura, P. Peng, K. Liu, M. Daou, and P. K. Srivastava, "Immunotherapy of tumors with autologous tumor-derived heat shock protein preparations," *Science*, vol. 278, no. 5335, pp. 117–120, 1997.
- [17] D. D. Mosser, A. W. Caron, L. Bourget, C. Denis-Larose, and B. Massie, "Role of the human heat shock protein hsp70 in protection against stress-induced apoptosis," *Molecular and Cellular Biology*, vol. 17, no. 9, pp. 5317–5327, 1997.
- [18] Y. Tamura and N. Sato, "Heat shock proteins: chaperoning of innate and adaptive immunities," *Japanese Journal of Hyperthermic Oncology*, vol. 19, pp. 131–139, 2003.
- [19] P. K. Srivastava, "Immunotherapy for human cancer using heat shock protein-peptide complexes," *Current Oncology Reports*, vol. 7, no. 2, pp. 104–108, 2005.
- [20] S. Takashima, N. Sato, A. Kishi, et al., "Involvement of peptide antigens in the cytotoxicity between 70-kDa heat shock cognate protein-like molecule and CD3⁺, CD4⁻, CD8⁻, TCR⁻ - killer T cells," *The Journal of Immunology*, vol. 157, no. 8, pp. 3391–3395, 1996.
- [21] M. Yanase, M. Shinkai, H. Honda, T. Wakabayashi, J. Yoshida, and T. Kobayashi, "Antitumor immunity induction by intracellular hyperthermia using magnetite cationic liposomes," *Japanese Journal of Cancer Research*, vol. 89, no. 7, pp. 775–782, 1998.
- [22] G. Ueda, Y. Tamura, I. Hirai, et al., "Tumor-derived heat shock protein 70-pulsed dendritic cells elicit-tumor-specific cytotoxic T lymphocytes (CTLs) and tumor immunity," *Cancer Science*, vol. 95, no. 3, pp. 248–253, 2004.
- [23] A. Ito, H. Honda, and T. Kobayashi, "Cancer immunotherapy based on intracellular hyperthermia using magnetite nanoparticles: a novel concept of "heat-controlled necrosis" with heat shock protein expression," *Cancer Immunology, Immunotherapy*, vol. 55, no. 3, pp. 320–328, 2006.
- [24] H. Shi, T. Cao, J. E. Connolly, et al., "Hyperthermia enhances CTL cross-priming," *The Journal of Immunology*, vol. 176, no. 4, pp. 2134–2141, 2006.
- [25] A. Ito, M. Fujioka, T. Yoshida, et al., "4-S-cysteaminylphenol-loaded magnetite cationic liposomes for combination therapy of hyperthermia with chemotherapy against malignant melanoma," *Cancer Science*, vol. 98, no. 3, pp. 424–430, 2007.
- [26] M. Sato, T. Yamashita, M. Ohkura, et al., "N-propionyl-cysteaminylphenol-magnetite conjugate (NPrCAP/M) is a nanoparticle for the targeted growth suppression of melanoma cells," *The Journal of Investigative Dermatology*, vol. 129, no. 9, pp. 2233–2241, 2009.
- [27] A. A. Brozyna, L. VanMiddlesworth, and A. T. Slominski, "Inhibition of melanogenesis as a radiation sensitizer for melanoma therapy," *International Journal of Cancer*, vol. 123, no. 6, pp. 1448–1456, 2008.
- [28] A. Slominski, B. Zbytek, and R. Slominski, "Inhibitors of melanogenesis increase toxicity of cyclophosphamide and lymphocytes against melanoma cells," *International Journal of Cancer*, vol. 124, no. 6, pp. 1470–1477, 2009.
- [29] M. Suzuki, M. Shinkai, H. Honda, and T. Kobayashi, "Anti-cancer effect and immune induction by hyperthermia of malignant melanoma using magnetite cationic liposomes," *Melanoma Research*, vol. 13, no. 2, pp. 129–135, 2003.
- [30] A. Ito, M. Shinkai, H. Honda, T. Wakabayashi, J. Yoshida, and T. Kobayashi, "Augmentation of MHC class I antigen presentation via heat shock protein expression by hyperthermia," *Cancer Immunology, Immunotherapy*, vol. 50, no. 10, pp. 515–522, 2001.
- [31] K. Jimbow, T. Takada, M. Sato, et al., "Melanin biology and translational research strategy: melanogenesis and nanomedicine as the basis for melanoma-targeted DDS and chemothermo-immunotherapy," *Pigment Cell and Melanoma Research*, vol. 21, no. 2, p. 243, 2008.
- [32] K. Jimbow, Y. Miyake, K. Homma, et al., "Characterization of melanogenesis and morphogenesis of melanosomes by physicochemical properties of melanin and melanosomes in malignant melanoma," *Cancer Research*, vol. 44, no. 3, pp. 1128–1134, 1984.
- [33] Y. Minamitsuji, K. Toyofuku, S. Sugiyama, and K. Jimbow, "Sulphur containing tyrosinase analogs can cause selective melanocytotoxicity involving tyrosinase-mediated apoptosis," *The Journal of Investigative Dermatology*, vol. 4, no. 2, pp. 130S–136S, 1999.
- [34] Y. Osai, M. Ohkura, Y. Tamura, et al., "Intratumoral administration of melanoma targeting N-propionyl cysteaminyphenol induces in vivo anti-melanoma effect and tumor specific immunity," *Pigment Cell & Melanoma Research*, vol. 21, no. 2, p. 329, 2008.

Aberrant expression and potency as a cancer immunotherapy target of alpha-methylacyl-coenzyme A racemase in prostate cancer

Ichiya Honma^{1,2}, Toshihiko Torigoe*¹, Yoshihiko Hirohashi¹, Hiroshi Kitamura², Eiji Sato², Naoya Masumori², Yasuaki Tamura¹, Taiji Tsukamoto² and Noriyuki Sato¹

Address: ¹Department of Pathology, Sapporo Medical University School of Medicine, Sapporo, Japan and ²Department of Urology, Sapporo Medical University School of Medicine, Sapporo, Japan

Email: Ichiya Honma - ichiya@sapmed.ac.jp; Toshihiko Torigoe* - torigoe@sapmed.ac.jp; Yoshihiko Hirohashi - hirohash@sapmed.ac.jp; Hiroshi Kitamura - hkitamu@sapmed.ac.jp; Eiji Sato - eiji@sapmed.ac.jp; Naoya Masumori - masumori@sapmed.ac.jp; Yasuaki Tamura - yamura@sapmed.ac.jp; Taiji Tsukamoto - taijit@sapmed.ac.jp; Noriyuki Sato - nsatou@sapmed.ac.jp

* Corresponding author

Published: 9 December 2009

Received: 29 January 2009

Accepted: 9 December 2009

Journal of Translational Medicine 2009, **7**:103 doi:10.1186/1479-5876-7-103

This article is available from: <http://www.translational-medicine.com/content/7/1/103>

© 2009 Honma et al; licensee BioMed Central Ltd.

This is an Open Access article distributed under the terms of the Creative Commons Attribution License (<http://creativecommons.org/licenses/by/2.0>), which permits unrestricted use, distribution, and reproduction in any medium, provided the original work is properly cited.

Abstract

Alpha-methylacyl-CoA racemase (AMACR) is an enzyme playing an important role in the beta-oxidation of branched-chain fatty acids and fatty acid derivatives. High expression levels of AMACR have been described in various cancers, including prostate cancer, colorectal cancer and kidney cancer. Because of its cancer-specific and frequent expression, AMACR could be an attractive target for cytotoxic T-lymphocyte (CTL)-based immunotherapy for cancer. In the present study, we examined the induction of AMACR-specific CTLs from prostate cancer patients' peripheral blood mononuclear cells (PBMCs) and determined HLA-A24-restricted CTL epitopes.

RT-PCR and immunohistochemical analysis revealed that AMACR was strongly expressed in prostate cancer cell lines and tissues as compared with benign or normal prostate tissues. Four AMACR-derived peptides carrying the HLA-A24-binding motif were synthesized from the amino acid sequence of this protein and analyzed to determine their binding affinities to HLA-A24. By stimulating patient's PBMCs with the peptides, specific CTLs were successfully induced in 6 of 11 patients. The peptide-specific CTLs exerted significant cytotoxic activity against AMACR-expressing prostate cancer cells in the context of HLA-A24. Our study demonstrates that AMACR could become a target antigen for prostate cancer immunotherapy, and that the AMACR-derived peptides might be good peptide vaccine candidates for HLA-A24-positive AMACR-expressing cancer patients.

Introduction

Cytotoxic T lymphocytes (CTLs) play a major role in the anti-cancer immune response [1]. Thus far, large numbers of tumor-associated antigens and their CTL epitopes have

been identified [2,3]. High-throughput gene expression profiling using a cDNA microarray allows for systematic interrogation of transcriptionally altered genes. By comparing the mRNA expression profiles of cancerous lesions

with non-cancerous lesions, a number of candidate antigens for tumor-specific immunotherapy have emerged. CTL epitope peptides derived from tumor-specific antigens like the MAGE gene family have been employed for pioneering studies of immunotherapy in cases of advanced melanoma patients [4,5].

Castration-resistant prostate cancer is an aggressive disease with limited treatment options. Hence, there is great need for new therapeutic strategies to treat prostate cancer, and recent progress in understanding of tumor immunology has raised expectations that antigen-specific immunotherapy may become a new modality for cancer therapy. Alpha-methylacyl coenzyme A racemase (AMACR) was identified as one of the genes that were highly expressed in prostate cancer tissues through gene expression profiling using a DNA microarray and RT-PCR [6-8]. AMACR is an enzyme that catalyzes the racemization of alpha-methyl carboxylic coenzyme A thioesters in mitochondria and peroxisomes [9,10]. AMACR is expressed abundantly in prostate cancer tissues as well as colorectal cancer and lung cancer tissues, whereas it is barely detected in benign tissues and normal prostate epithelial cells [6-8]. Immunohistochemical staining for AMACR is currently used in the clinical setting to support the histological diagnosis of prostate cancer. Because it has characteristics of cancer-specific expression and frequent expression in various cancers, AMACR is an attractive target for cancer immunotherapy. In the present study, we examined the induction of AMACR-specific CTLs from prostate cancer patients' peripheral blood mononuclear cells (PBMCs) and determined HLA-A24-restricted CTL epitopes. Our study demonstrates for the first time HLA-A24-restricted AMACR-derived CTL epitopes that might be suitable for peptide vaccines for AMACR-expressing cancer patients.

Materials and methods

Tissue Samples and PBMC

Surgically resected tissue specimens and PBMCs were obtained from HLA-A*2402-positive prostate cancer patients who were treated at Sapporo Medical University Hospital (Sapporo, Japan) after obtaining their informed consent. The study was approved by the Institutional Review Board for Clinical Research at our university. The expression of HLA-A24 molecules on PBMCs of cancer patients was determined by flow cytometry using an anti-HLA-A24 monoclonal antibody (c7709A2.6, kindly provided by Dr. P. G. Coulie, Ludwig Institute for Cancer Research, Brussels Branch).

Cell Lines and Culture

Prostate cancer cell lines (LNCaP, DU145, and PC-3) and proerythroleukemia cell line K562 were cultured in RPMI 1640 (Sigma, St. Louis, MO) supplemented with 10%

fetal bovine serum (FBS) (Filtron, Brooklyn, Australia). T2-A*2402 cells, which are transporters associated with antigen processing (TAP)-deficient T2 cells transfected with HLA-A*2402 complementary DNA (cDNA) were cultured in RPMI 1640 supplemented with 10% fetal bovine serum and 800 I g/mL G418 (Invitrogen Life Technologies Co., Carlsbad, CA). LNCaP and DU145 are HLA-A*2402-negative prostate cancer cell lines. To generate LNCaP and DU-145 sublines expressing HLA-A24, HLA-A*2402 cDNA was transfected into the cells by electroporation using a Gene Pulser (Bio-Rad, Richmond, CA) as reported previously [11]. The expression of HLA-A24 molecules on the cell lines was determined by flow cytometry using the anti-HLA-A24 monoclonal antibody. LNCaP-A*2402 and DU145-A*2402, stable HLA-A*2402 transfectants of LNCaP and DU145 cells, respectively, were established and cultured in RPMI 1640 supplemented with 10% FBS and 500 ng/ml puromycin (Sigma).

Reverse transcriptase-polymerase chain reaction (RT-PCR)

Multiple Tissue cDNA Panels (BD Biosciences Clontech, Palo Alto, CA) were used as a template of normal tissue cDNA. Total RNA was extracted using an RNeasy kit (Qiagen, Hilden, Germany). A cDNA mixture was synthesized from 1 I g of total RNA by reverse transcription (RT) using Superscript II and oligo (dT) primer (Invitrogen Life Technologies) according to the manufacturer's protocol. PCR amplification was done in 50 I L of PCR mixture containing 1 I L of the cDNA mixture, 1 I L of KOD Plus DNA polymerase (TOYOBO, Osaka, Japan) and 15 pmol of primers. For specific detection of AMACR, forward primer 5'-CGG GGT ACC ATG GCA CTG CAG GGC ATC TCG-3' and reverse primer 5'-ATA AGA ATG CGG CCG CGA GAC TAG CTT TTA CCT TAT TAC T-3' were employed. As an internal control, β -actin expression was detected by using forward primer 5'-ACT GGC TCG TGA TGG ACT C-3' and reverse primer 5'-TCA GGC AGC TCG TAG CTC TT-3'. The amplification protocol consisted of denaturation for 15 seconds at 98°C, annealing for 45 seconds at 58°C and extension for 4 minutes at 72°C for a total of 30 cycles, using a GeneAmp PCR system model 2400 (Perkin-Elmer, Foster City, CA).

Immunohistochemical Staining of Tissue Sections

Immunohistochemical staining was done with formalin-fixed paraffin-embedded tissue sections of surgically resected prostate cancer specimens. Four- to 5-I m-thick sections were deparaffinized in xylene and rehydrated in graded alcohols. Antigen retrieval was done by boiling sections for 20 minutes in a microwave oven in preheated 0.01 mol/L sodium citrate buffer (pH 6.0). Endogenous peroxidase activity was blocked by 3% hydrogen peroxide in ethanol for 10 minutes. After blocking with 1% non-fat dry milk in phosphate-buffered saline (PBS) (pH 7.4), the

sections were reacted with a rabbit polyclonal antibody to AMACR (clone RP134, Diagnostic BioSystems Co., Pleasanton, CA, USA) at 25 I g/mL or preimmune sera for 1 hour, followed by incubation with biotinylated goat anti-rabbit IgG (Nichirei, Tokyo, Japan) for 30 minutes. Subsequently, the sections were stained with streptavidin-biotin complex (Nichirei), followed by incubation with 3,3'-diaminobenzidine and counterstaining with hematoxylin. The same tissues were immunostained with an anti-prostate-specific antigen (PSA) polyclonal antibody (DAKO, Denmark).

Peptides and Cytokines

AMACR-derived peptides were synthesized from the amino acid sequence of AMACR based on the HLA-A24-binding motifs. AMACR-derived peptides were provided by Dainippon Sumitomo Pharmaceutical Co. (Osaka, Japan). Two peptides were used as control peptides, Epstein-Barr virus (EBV) LMP2-derived peptide (TYG-PVFMSL) and human immunodeficiency virus (HIV) env-derived peptide (RYLRDQQLGI), which have been shown to become CTL epitopes in the context of HLA-A*2402 previously [12,13], and ovalbumin-derived SL-8 peptide (OVA257-264, SIINFEKL) was used as a negative control peptide. These peptides were synthesized and purchased from Sigma Genosys (Ishikari, Japan). The peptides were dissolved in DMSO at a concentration of 5 mg/mL and stored at -80°C. Human recombinant interleukin (IL)-2, IL-4 and granulocyte macrophage colony-stimulating factor (GM-CSF) were kind gifts from Takeda Pharmaceutical Co. (Osaka, Japan), Ono Pharmaceutical Co. (Osaka, Japan) and Novartis Pharmaceutical (Basel, Switzerland), respectively. Human recombinant IL-7 was purchased from Invitrogen Life Technologies.

Peptide Binding Assay

Peptide binding affinity to the HLA-A24 molecule was assessed by HLA-A24 stabilization assay as described previously [13], based on the findings that MHC class I molecules could be stabilized on the cell surface in the presence of binding peptides. After incubation of T2-A*2402 cells in culture medium at 26°C for 18 hours, the cells (2×10^5) were washed with PBS and suspended with 1 mL of Opti-MEM (Life Technologies) with or without 100 I g of peptide, followed by incubation at 26°C for 3 hours and then at 37°C for 3 hours. After washing with PBS, the cells were incubated with the anti-HLA-A24 monoclonal antibody at 4°C for 30 minutes, followed by incubation with fluorescein isothiocyanate (FITC)-conjugated rabbit anti-mouse IgG at 4°C for 30 minutes. The cells were then suspended with 1 mL of PBS containing 1% formaldehyde, and analyzed by FACScan (Becton Dickinson, Mountain View, CA). Binding affinity was evaluated by comparing mean fluorescence intensity (MFI) of HLA-

A24 expression in the presence of peptide pulsation to MFI in the absence of the peptide.

Peptide-specific CTL Induction with Immature Dendritic Cells and Phytohemagglutinin Blasts

PBMCs were isolated from prostate cancer patients by standard density gradient centrifugation on Lymphoprep (Nycomed, Oslo, Norway). PBMCs were incubated in AIM-V medium (Invitrogen Life Technologies, Inc.) supplemented with 2-mercaptoethanol (50 I M) and HEPES (10 mM) for 2 hours at 37°C in a culture flask to separate adherent cells and non-adherent cells. Adherent cells were then cultured in the presence of IL-4 (1000 units/ml) and GM-CSF (1000 units/ml) in AIM-V medium for 7 days to generate monocyte-derived dendritic cells (DCs). The adherent cells containing DCs and phytohemagglutinin (PHA)-stimulated blasts were used as antigen-presenting cells (APCs). CD8-positive T lymphocytes were isolated from non-adherent cells with the MACS separation system (Milteny Biotech, Bergish Blabach, Germany) using an anti-CD8 monoclonal antibody coupled with magnetic microbeads according to the manufacturer's instructions. To obtain PHA-stimulated blasts, CD8-negative non-adherent PBMCs were cultured in AIM-V medium containing 1 I g/ml PHA (WAKO Chemicals, Osaka, Japan) and 100 units/ml of IL-2 for 3 days, followed by washing and cultivation in the presence of IL-2 (100 units/ml) for 4 days.

CTLs were induced from PBMCs of cancer patients by using autologous DC and PHA-blasts as APCs as described previously [14,15]. Briefly, APCs were cultured in AIM-V medium supplemented with 50 I mol/L peptide at room temperature for 2 hours, followed by washing with AIM-V once, then irradiated (100 Gy) and used for stimulation of CTLs. The CTL induction procedure was initiated by stimulating CD8⁺ cells with peptide-pulsed autologous DCs at a 20:1 effector/APC ratio in AIM-V supplemented with HEPES, 2-ME, and IL-7 (10 ng/mL) for 7 days at 37°C. The following stimulation was done with peptide-pulsed PHA-blasts at a 10:1 effector/APC ratio. On the day after the 2nd stimulation, IL-2 was added to the culture at a concentration of 10 units/mL. The same CTL stimulation cycle with PHA-blasts was then done twice more over a period of 2 weeks. One week after the 4th stimulation, cytotoxic activity of the CTL was measured by ⁵¹Cr release assay.

Cytotoxicity Assay

The cytotoxic activities of CTLs were measured by ⁵¹Cr-release assay as described previously [16]. Target cells were labeled with 100 I Ci of ⁵¹Cr for 1 hour at 37°C and washed with RPMI 1640 three times. Then ⁵¹Cr-labeled target cells were incubated with or without peptide and effector cells at various effector/target ratios at 37°C for 6

hours in V-bottomed 96-well microtiter plates. Then supernatants were collected and the radioactivity was measured with a gamma-counter. The % specific lysis was calculated as follows: % specific lysis = (test sample release - spontaneous release) × 100/(maximum release - spontaneous release). For peptide-pulsed target cells, T2-A*2402 cells were incubated with 1 I g/ml peptide at room temperature for 1 hour before the assay. Moreover, we also examined cytotoxic activity against LNCaP, LNCaP-A*2402, DU145 and DU145-A*2402 prostate cancer cells, which express endogenous AMACR.

ELISPOT Assay

ELISPOT plates were coated sterilely overnight with an IFN- γ capture antibody (Beckton Dickinson Biosciences) at 4°C. The plates were then washed once and blocked with AIM-V medium containing 10% human serum for 2 hr at room temperature. CD8-positive T cells separated from patients' PBMCs (5×10^3 cells/well), which were stimulated *in vitro* with peptides, were then added to each well along with HLA-A24-transfected CIR cells (CIR-A24) (5×10^4 cells/well), which had been preincubated with the AMACR peptide (10 I g/ml) or HIV peptide as a negative control. After incubation in a 5% CO₂ humidified chamber at 37°C for 24 hours, the wells were washed vigorously five times with PBS and incubated with a biotinylated anti-human IFN- γ antibody and horseradish peroxidase-conjugated avidin. Spots were visualized and analyzed using KS ELISPOT (Carl Zeiss, Germany).

Statistical Analysis

We tested the statistical significance of cytotoxic activity of CTLs induced with peptides using Student's t-test. A value of $p < 0.05$ was considered to indicate statistical significance.

Results

AMACR Expression in Normal Tissues, Prostate Cancer Cell Lines and Cancer Tissues

First the expression profile of AMACR in normal adult tissues by RT-PCR was defined. We detected the overt expression of β -actin mRNA and AMACR mRNA in prostate cancer line LNCaP, but only very weak expression of AMACR mRNA was observed in normal adult liver and pancreas (Figure 1A). In contrast, the AMACR mRNA level was elevated in all three prostate cancer cell lines (LNCaP, DU145 and PC-3) and in surgically resected prostate cancer tissues (Figure 1B and 1C). Low levels of expression were detected in non-cancerous prostate tissues (Figure 1C).

Immunohistochemical analysis revealed that AMACR was present in prostate cancer tissues in 27 (69.2%) of the 39 patients (Figures 2A and 2B). AMACR was weakly detected in non-cancerous prostate tissues, but barely detected in

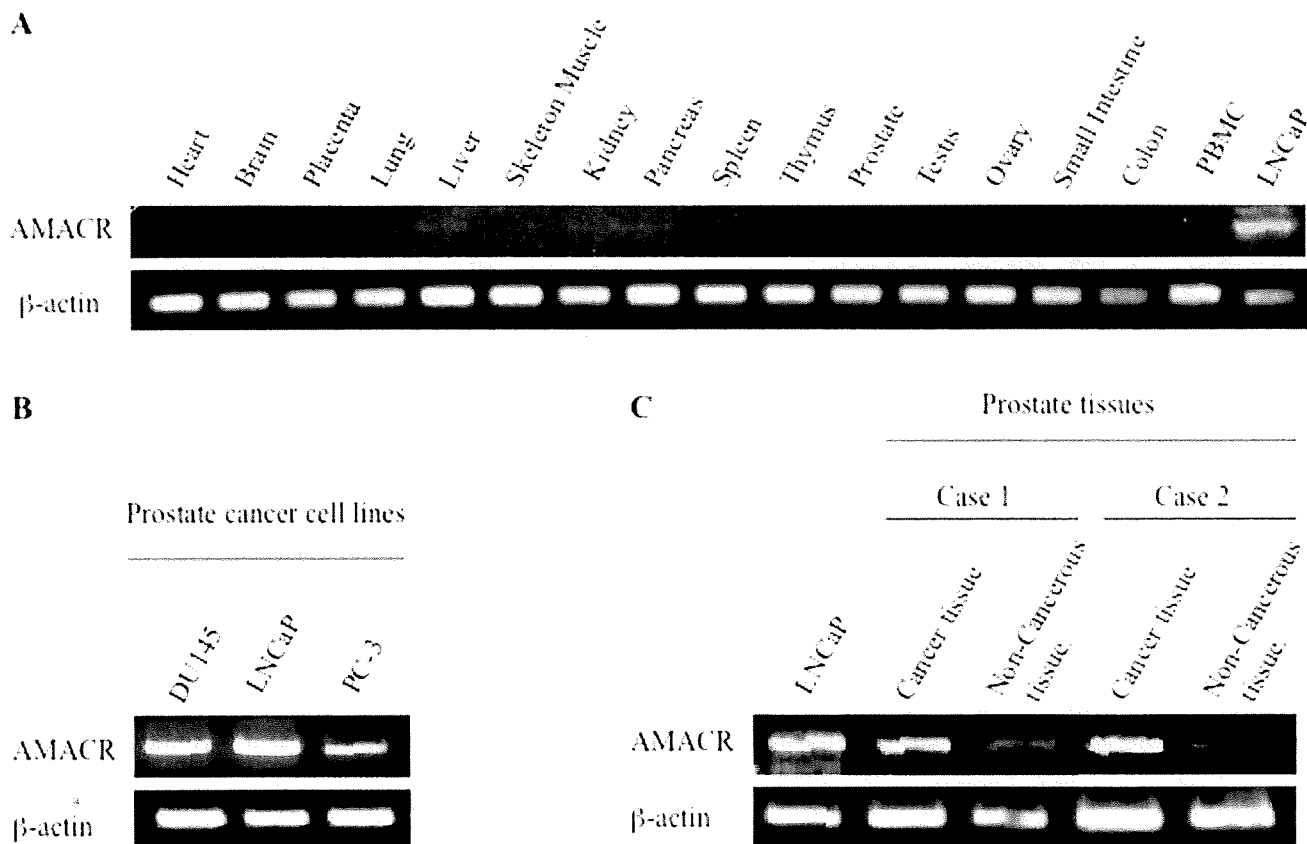
normal essential tissues such as adult liver and pancreas by immunohistochemical staining. In contrast, PSA was stained in both prostate cancer tissue and non-cancerous tissue (Figure 2C). These data indicated that AMACR had a mostly cancer-specific expression profile at both the mRNA level and protein levels.

AMACR-derived Peptides Carrying HLA-A24 Binding Motif

Antigenic peptides derived from AMACR protein might be presented by HLA class I molecules and recognized by CD8-positive T cells. We focused on HLA-A*2402-restricted peptides because of its high frequency in Asian people. The amino acid sequence of AMACR protein was screened for peptides that had an HLA-A24 binding motif, such as 9- and 10-mer peptides with Y, F, M, or W at the 2nd position and L, I, F, or M at COOH-terminal position [17]. Consequently, we found four peptides, AMACR1 (NYLALSGVL), AMACR2 (NMVEGTAYL), AMACR3 (FYELLIKGL) and AMACR4 (IYQLNSDKII) carrying the HLA-A24 binding motif (Figure 3A). Next, we assessed their binding affinities to HLA-A24 molecules by a binding assay using TAP-deficient T2 cells transfected with HLA-A*2402. The MFI of cell surface HLA-A24 was clearly increased in the presence of positive control peptides, EBV peptide and HIV peptide, whereas it was not changed in the presence of negative control peptide SL-8, indicating the adequate qualification of this assay. The HLA-A24 level on the cell surface of T2-A*2402 cells was up-regulated in the presence of AMACR1, AMACR2 and AMACR3 peptides, but not in the presence of AMACR4 peptide, indicating that AMACR1, 2 and 3 peptides were possible HLA-A24-presentable peptides (Figure 3B).

CTL Induction from PBMCs of HLA-A24-positive Prostate Cancer Patients

We attempted to induce AMACR peptide-specific CTLs from PBMCs of HLA-A24 positive prostate cancer patients and assessed their cytotoxic activity. PBMCs were cultured with APCs pulsed with a mixture of three AMACR-derived peptides. After stimulation four times with the peptides, the cytotoxic activity against peptide-pulsed target cells was examined by ⁵¹Cr-release assay. The CTLs induced by the *in vitro* stimulation with AMACR peptides showed specific reactivity to the peptide-pulsed T2-A*2402 cells in 6 of 11 cases of HLA-A24-positive patients with AMACR-positive prostate cancer (Table 1 and Figures 4, 5, 6 and 7). CTLs could not be induced in any of the patients with AMACR-negative prostate cancer. In five cases (cases 1, 2, 3, 5 and 6) with AMACR-positive prostate cancer, CTLs reacting to AMACR2 peptide-pulsed T2-A*2402 cells were induced (Figure 5). With respect to AMACR1 and the 3 peptides, peptide-specific CTLs were induced in three cases (cases 4, 5 and 6, Figure 4) and two cases (cases 5 and 6, Figure 6), respectively. Since the cytotoxic activity of CTLs of case 6 was relatively low as compared with the

**Figure 1**

Expression profiles of AMACR as assessed by RT-PCR. A. Expression of AMACR in normal tissues including heart, brain, placenta, lung, liver, skeletal muscle, kidney, pancreas, spleen, thymus, prostate, testis, ovary, small intestine, colon and PBMC. LNCaP, a prostate cancer cell line was used as a positive control for AMACR expression. B. Expression of AMACR in prostate cancer cell lines. Beta-actin expression was detected as an internal control. AMACR mRNA was detected in three prostate cancer cell lines (LNCaP, DU145 and PC-3). C. Expression of AMACR in cancer tissues and noncancerous tissues from surgical specimens of two prostate cancer cases.

other cases, peptide-specificity was assessed by ELISPOT assay. CTLs of case 6 could release interferon- γ in response to AMACR1, 2 and 3 peptides, but not in response to AMACR4 peptide or HIV peptide (Figure 7), indicating that the peptide specificity of the CTLs was consistent with the cytotoxic assay.

Cytotoxic Activity of AMACR Peptide-specific CTLs Against HLA-A24-positive AMACR-positive Prostate Cancer Cell Lines

To confirm that CTLs induced with AMACR peptides could exert cytotoxicity against AMACR-expressing prostate cancer cell lines in an HLA-A*2402-restricted manner, we examined their cytotoxic activity against prostate cancer cell lines that express endogenous AMACR by ^{51}Cr -release assay. LNCaP-A*2402 and DU145-A*2402, which express both endogenous AMACR and gene-transfected

HLA-A*2402, were used as target cells. Parental LNCaP and DU145 cells, HLA-A*2402-negative prostate cancer cells, were used as negative control target cells. As shown in Figure 8, CTLs induced from PBMCs of HLA-A*2402-positive prostate cancer patients (cases 3, 4 and 5) with AMACR peptides exerted cytotoxic activity against LNCaP-A*2402 and DU145-A*2402 cells but not against LNCaP and DU145 cells. These data implied that the peptide-specific CTLs were capable of recognizing endogenously processed AMACR-derived peptides in an HLA-A24-restricted manner.

Discussion

Specific immunotherapy for cancer is anticipated to become an alternative or complementary therapy for recurrent or metastatic disease. Successful immunotherapy depends on the identification of cancer-specific

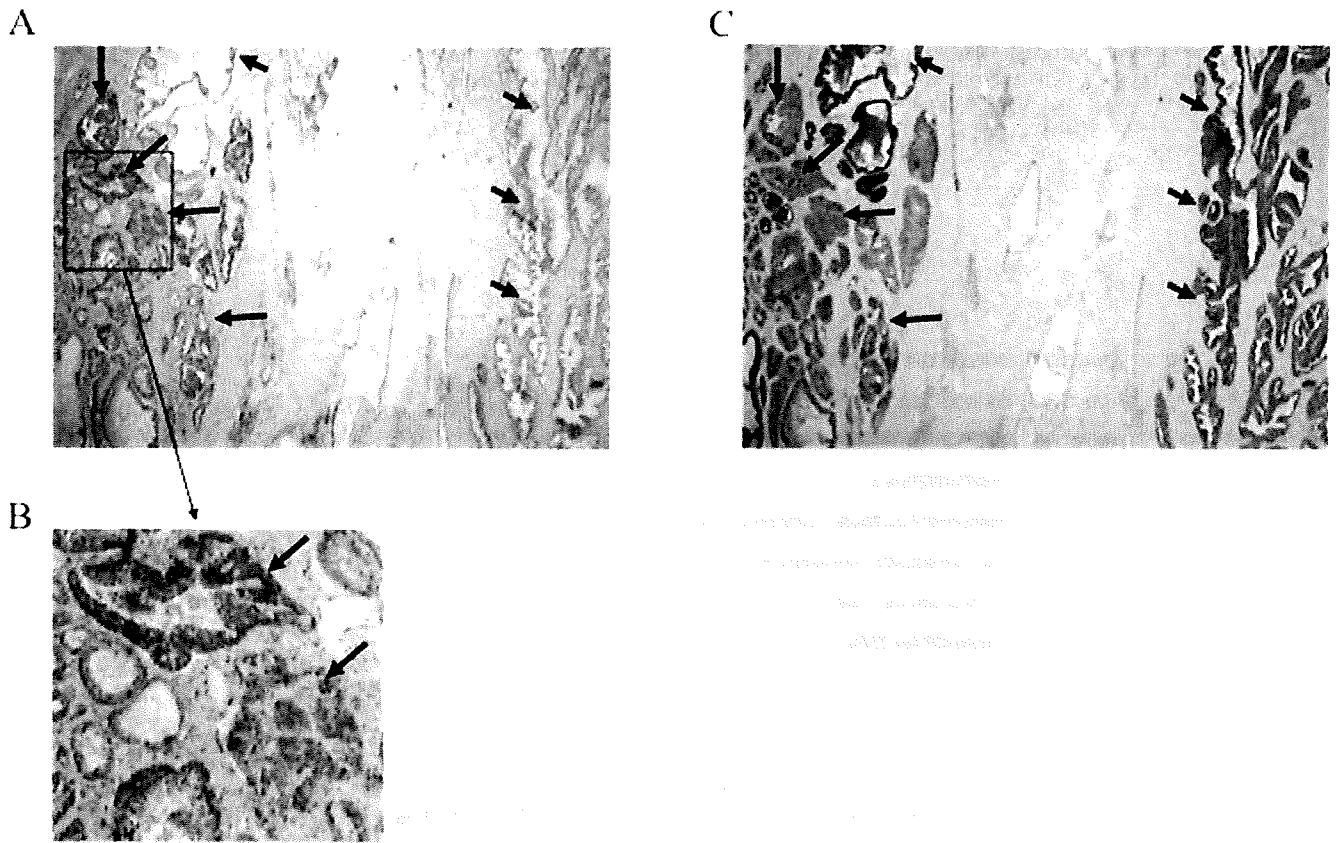


Figure 2

Immunostaining of prostate cancer tissue with antibodies against AMACR and PSA. Surgically resected prostate cancer tissue was immunostained with an anti-AMACR antibody (panel A) or anti-PSA antibody (panel C). The lower column (panel B) is a magnified view of the box of panel A. A clear distinction is noted between cancerous tissue with strongly positive AMACR staining (long arrow) and noncancerous glands without AMACR staining (short arrow) whereas both of them are positive for PSA.

antigens and the immunopotent CTL epitopes. Proteins that are selectively expressed in cancer cells, but not in normal adult tissues should become suitable targets for cancer-specific immunotherapy. To establish effective immunotherapy for prostate cancer, exploration of prostate cancer-specific antigens has been conducted.

Although prostate-specific antigen (PSA) is a well-known serum biomarker for prostate cancer, it has poor specificity to cancer. PSA is highly expressed in noncancerous prostatic tissues as well as in cancerous tissues [18-20] as shown in Figure 2B in the present study. Indeed, serum PSA levels are increased in patients with benign prostatic diseases such as benign prostatic hypertrophy and prostatitis. Recently, new prostate cancer antigens have been reported and examined as target antigens for cancer-specific immunotherapy [21-23]. In the present study, we focused on AMACR, a novel antigen that is overexpressed in a variety of tumor tissues, including prostate cancer.

AMACR was identified as a tissue biomarker for prostate cancer by gene expression profiling of primary human prostate cancer and benign prostatic hyperplasia (BPH) using cDNA microarrays [8]. Initial studies reported that AMACR was overexpressed in 94-100% of prostate cancers [6-8] though recent studies have demonstrated a slightly lower expression rate in the range of 80-90% for prostate cancer [24-26]. In our study, AMACR was detected in about 70% of prostate cancer cases by immunohistochemical analysis. This frequency was slightly lower than those of previous reports. On the other hand, its expression was very low in benign prostate glands, which showed only focal and weak staining [6]. The function of AMACR in prostate cancer has not been clarified yet. It has been reported that the function and expression of AMACR might be independent of androgen receptor signaling [27]. Recently, it has been reported that AMACR is overexpressed in various tumor tissues, including renal cell cancer, hepatic cancer, colon cancer and lung cancer.

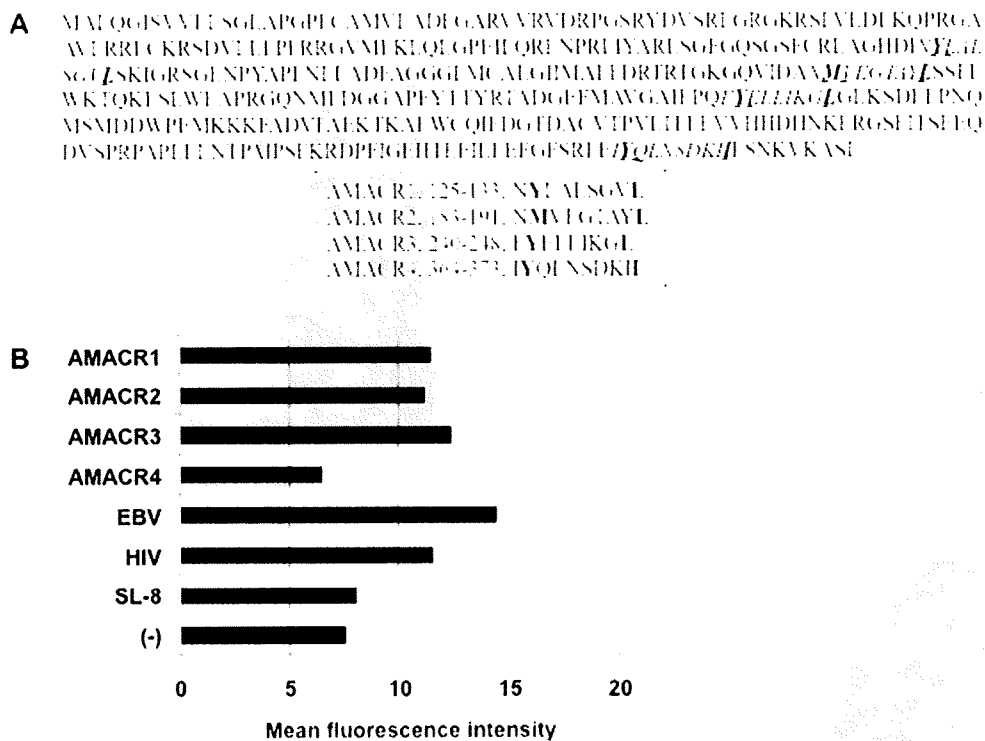


Figure 3

Amino acid sequences of AMACR-derived peptides and their HLA-A24 binding assay. A. Amino acid sequences of AMACR protein and four peptides (AMACR1-4) with HLA-A24 binding motif (underlines). The predicted anchor residues to HLA-A24 are indicated in boldface within the amino acid sequences of the peptides. B Binding affinities of AMACR-derived peptides to HLA-A24 molecule were evaluated by the mean fluorescence intensity (MFI) of cell surface HLA-A24 molecules on T2-A*2402 cells that were pulsed with each peptide. EBV LMP2-derived peptide (TYGPVFM^SL) and HIV env-derived peptide (RYLRDQQLG^I) were used as positive controls for HLA-A24-bound peptides. SL-8 peptide (SIINFEK^L) was used as a negative control.

Table 1: Summary of clinicopathological characteristics and peptide-specific CTL induction from the peripheral blood mononuclear cells of prostate cancer patients

Case no.	Age (years old)	PSA (ng/ml)	Gleason score	Pathologic stage	AMACR expression	CTL induction	Peptide specificity
1	60	6.7	4+3	T2aN0M0	+	+	AMACR2
2	73	6.0	3+3	T2aN0M0	+	+	AMACR2
3	65	11.6	4+3	T2bN0M0	+	+	AMACR2
4	64	15.6	3+4	T3aN0M0	+	+	AMACR1
5	67	18.4	4+5	T3aN0M0	+	+	AMACR1,2,3
6	67	14.4	4+3	T2bN0M0	+	+	AMACR1,2,3
7	71	10.9	3+5	T3bN0M0	+	-	-
8	71	4.6	3+4	T2aN0M0	+	-	-
9	72	5.7	3+4	T2aN0M0	+	-	-
10	67	8.0	4+4	T2aN0M0	+	-	-
11	67	4.3	3+3	T2bN0M0	+	-	-
12	61	11.5	3+4	T2aN0M0	-	-	-
13	61	10.1	4+3	T2bN0M0	-	-	-
14	61	10.4	3+4	T2aN0M0	-	-	-
15	60	6.6	3+4	T2aN0M0	-	-	-

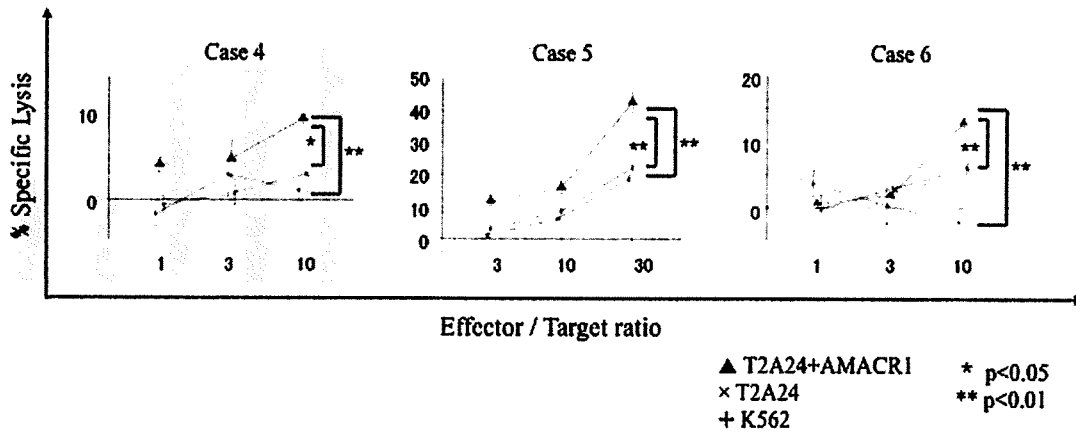


Figure 4
AMACR1 peptide-specific CTL induction from PBMCs of HLA-A24-positive prostate cancer patients. PBMCs of HLA-A24-positive prostate cancer patients (cases 4, 5 and 6) were stimulated four times with three kinds of AMACR peptide (AMACR1-3)-pulsed APCs and their cytotoxic activities were examined by ⁵¹Cr release assay at the indicated effector/target ratios. AMACR1 peptide-pulsed T2-A*2402 cells served as target cells. Non-pulsed T2-A*2402 cells were used as negative control target cells. K562 target cells were used for monitoring natural killer cell activity and lymphokine-activated nonspecific cytotoxicity.

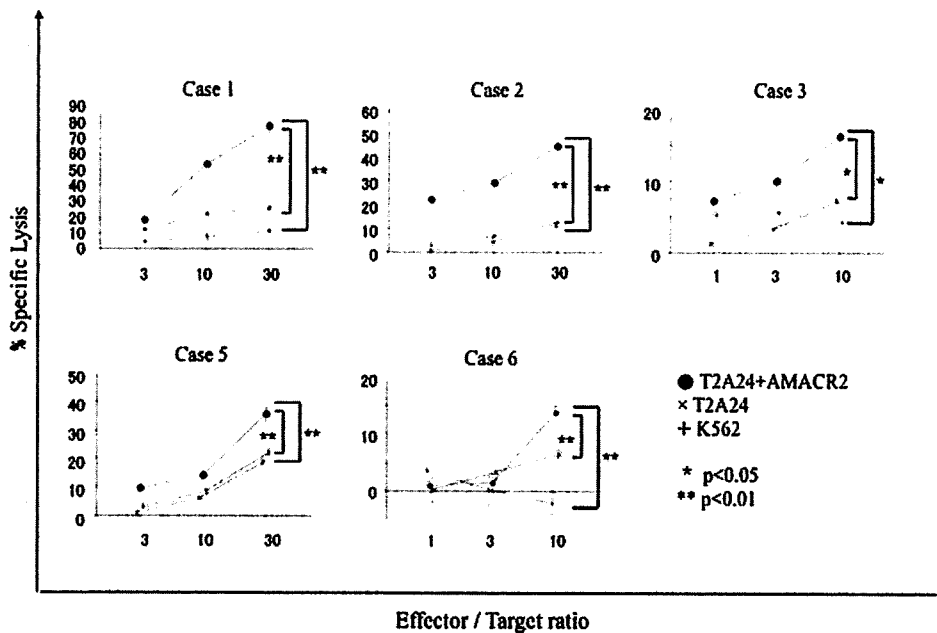


Figure 5
AMACR2 peptide-specific CTL induction from PBMCs of HLA-A24-positive prostate cancer patients. PBMCs of HLA-A24-positive prostate cancer patients (cases 1, 2, 3, 5 and 6) were stimulated four times with three kinds of AMACR peptide (AMACR1-3)-pulsed APCs and their cytotoxic activities were examined by ⁵¹Cr release assay at the indicated effector/target ratios. AMACR2 peptide-pulsed T2-A*2402 cells served as target cells. Non-pulsed T2-A*2402 cells and K562 cells were used as negative control target cells.